AD-A066 496 NAVAL POSTGRADUATE SCHOOL MONTEREY CALIF F/G 13/10
XR-3 BOW SEAL DIFFERENTIAL DRAG IN TURNS,(U)
DEC 78 D A EDWARDS

UNCLASSIFIED NL

| OF |
AD
AD66496

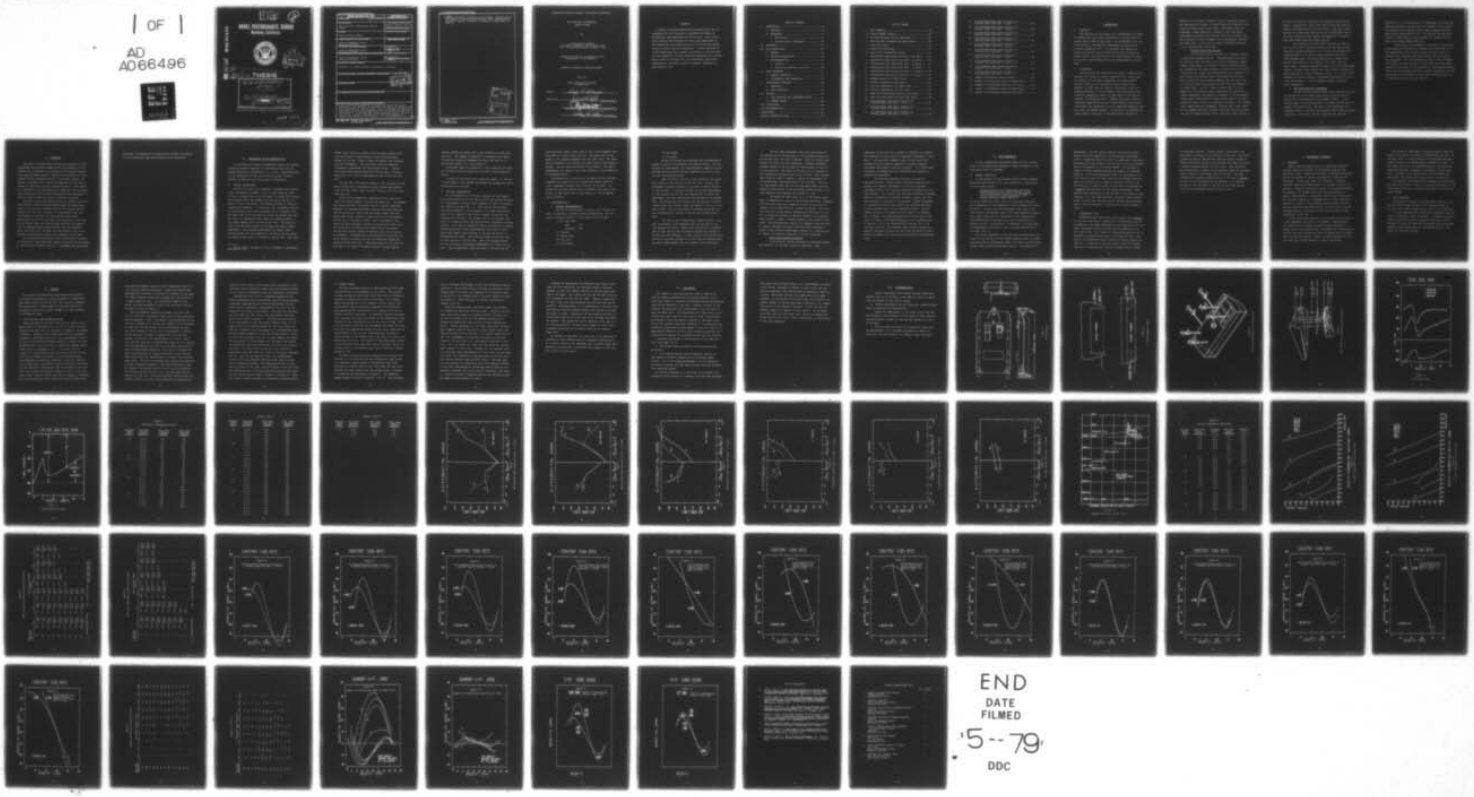

END
DATE FILMED
5-79
DDC

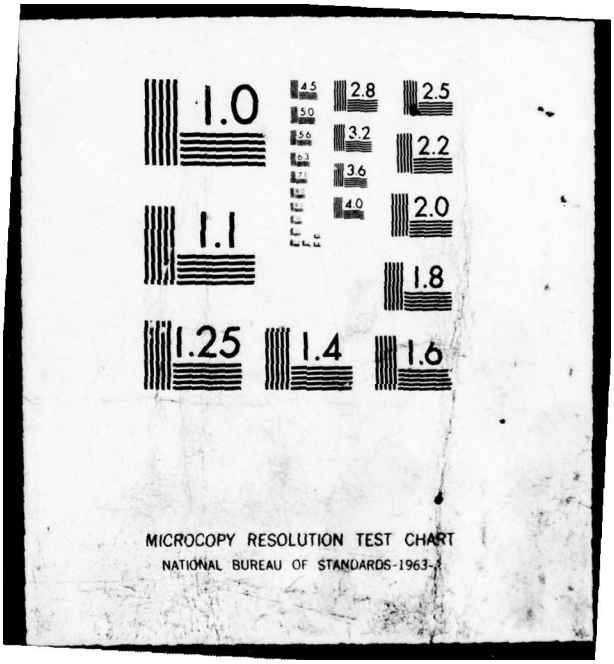
1.0
1.1
1.25
1.4
1.6
1.8
2.0
2.2
2.5
2.8
3.2
3.6
4.0
4.5
5.0
5.6
6.3
MICROCOPY RESOLUTION TEST CHART
NATIONAL BUREAU OF STANDARDS-1963-A

NAVAL POSTGRADUATE SCHOOL

Monterey, California

(9) Master's THESIS

(6) XR-3 BOW SEAL DIFFERENTIAL DRAG IN TURNS

by

(10) David Anthony Edwards

(11) Dec [redacted] 78

(12) 77 p.

Thesis Advisor: D.M. Layton

SECURITY CLASSIFICATION OF THIS PAGE (When Data Entered)

REPORT DOCUMENTATION PAGE		READ INSTRUCTIONS BEFORE COMPLETING FORM
1. REPORT NUMBER	2. GOVT ACCESSION NO.	3. RECIPIENT'S CATALOG NUMBER
4. TITLE (and Subtitle) XR-3 Bow Seal Differential Drag in Turns		5. TYPE OF REPORT & PERIOD COVERED Master's Thesis: Dec 78 6. PERFORMING ORG. REPORT NUMBER
7. AUTHOR(s) David Anthony Edwards		8. CONTRACT OR GRANT NUMBER(s)
9. PERFORMING ORGANIZATION NAME AND ADDRESS Naval Postgraduate School Monterey CA 93940		10. PROGRAM ELEMENT, PROJECT, TASK AREA & WORK UNIT NUMBERS
11. CONTROLLING OFFICE NAME AND ADDRESS Naval Postgraduate School Monterey CA 93940		12. REPORT DATE December 1978 13. NUMBER OF PAGES 76
14. MONITORING AGENCY NAME & ADDRESS(if different from Controlling Office) Naval Postgraduate School Monterey CA 93940		15. SECURITY CLASS. (of this report) Unclassified 15a. DECLASSIFICATION/DOWNGRADING SCHEDULE

16. DISTRIBUTION STATEMENT (of this Report)

Approved for public release; distribution unlimited.

17. DISTRIBUTION STATEMENT (of the abstract entered in Block 20, if different from Report)

18. SUPPLEMENTARY NOTES

19. KEY WORDS (Continue on reverse side if necessary and identify by block number)

20. ABSTRACT (Continue on reverse side if necessary and identify by block number)

A series of turning maneuvers was conducted with the instrumented XR-3 SES testcraft to determine the domain of differential drag experienced by the bow seal. Data is presented showing the difference in total drag experienced by the inboard and the outboard portions of the bow seal during turns at various testcraft velocities. A brief introduction to SES terminology and a summary description of the testcraft, its instrumentation and

DD FORM 1 JAN 73 1473 EDITION OF 1 NOV 65 IS OBSOLETE
S/N 0102-014-6601

SECURITY CLASSIFICATION OF THIS PAGE (When Data Entered)

and data reduction facilities are included. Results show a fluctuation of the differential drag forces experienced as testcraft velocity increases, especially at high rates of turn.

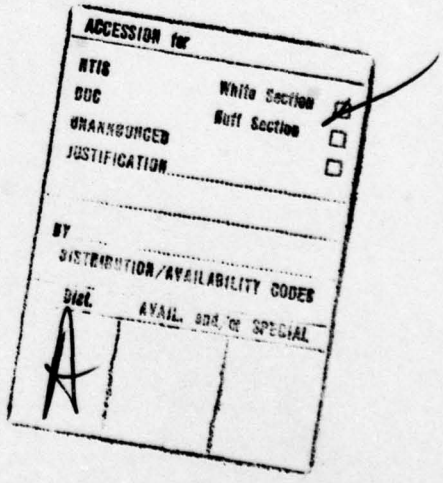

Approved for public release; distribution unlimited

XR-3 BOW SEAL DIFFERENTIAL DRAG IN TURNS

by

David Anthony Edwards
Lieutenant Commander, United States Navy
B.S., United States Naval Academy, 1968

Submitted in partial fulfillment of the
requirements of the degree of

MASTER OF SCIENCE IN APPLIED SCIENCE

from the

NAVAL POSTGRADUATE SCHOOL
December 1978

Author David A. Edwards

Approved by: Donald M. Layton
Thesis Advisor

R. J. Marto
Chairman, Department of Mechanical Engineering

William M. Tolles
Dean of Science and Engineering

ABSTRACT

A series of turning maneuvers was conducted with the instrumented XR-3 SES testcraft to determine the domain of differential drag experienced by the bow seal. Data is presented showing the difference in total drag experienced by the inboard and the outboard portions of the bow seal during turns at various testcraft velocities. A brief introduction to SES terminology and a summary description of the testcraft, its instrumentation and data reduction facilities are included. Results show a fluctuation of the differential drag forces experienced as testcraft velocity increases, especially at high rates of turn.

TABLE OF CONTENTS

LIST OF FIGURES

I. INTRODUCTION

A. OBJECTIVE

The objective of this report is to investigate the domain of differential drag forces experienced by the bow seal of a surface effect craft during turns. The investigation was conducted using an instrumented, experimental surface effect testcraft designated XR-3. The testcraft was operated at various velocities and turn rates and the data recorded to permit analysis and exposition of the relationship and ranges of the total differential drag forces experienced by the bow seal.

B. BACKGROUND

Vehicles which are lifted from the earth's surface by air pressure are called air cushion vehicles (ACV). These craft are divided into two basic categories; the ground effect vehicles (GEV) and the captured air bubble (CAB) craft. Briefly, the GEV's are the familiar "hovercraft" which are supported entirely on an air cushion, and consequently, are constantly pumping air under the lower edge of the vehicle's flexible, air-retaining skirt. Because the entire vehicle is completely supported by the air cushion several inches above the surface, the hovercraft is a true amphibian operating over both water and benign terrain. In contrast, the captured air bubble craft is used only in the water where, because of

immersion of the craft's sidewall hulls in the water, most of the supporting air cushion is indeed "captured" instead of constantly escaping under a skirt edge. While GEV's have the advantage of being amphibious, because of the lower power requirements associated with the CAB craft, much interest has been generated in the development of an ocean-going, captured air bubble ship. Such a ship is almost universally referred to as a Surface Effect Ship (SES).

1. Surface Effect Ship Concept

The SES rides across the water on a captured cushion of mechanically pressurized air. The pressurized air cushion is contained under the craft in a usually rectangular plenum chamber consisting of two parallel, vertical sidewalls partially immersed in the water surface on either side of the craft, a horizontal flat upper deck connecting the two sidewalls and two flexible air pressure seals (one forward and one aft). Each of these two seals extends downward from the upper deck to the water surface and across the craft from one sidewall to the other (Fig. 1 and 1a). When a large volume of air is pumped into this space by fans located atop the upper deck, a slight atmospheric overpressure is produced in the rectangular plenum which, acting over the large surface area of the deck, causes the craft to rise on a captured air bubble. The sidewall hulls remain partially submerged. Because only a small amount of air escapes the plenum (usually under the rear seal during the craft's forward motion), only a relatively small amount of

air must be replaced to maintain the supporting captured air bubble. Consequently, less of the craft's available power is used for the generation of the air cushion. The large, useful surface of the SES upper deck and the low hydrodynamic drag of the small underwater body combine advantageously to produce a high speed vessel with good cargo capacity.

The captured air bubble does not propel the SES; it must be fitted with separate propulsion and steering systems. Propulsion systems currently in use include the standard submerged propeller, the thrust of high pressure water jets, semi-submerged super cavitating propellers and simple deck-mounted fans similar to the familiar "air boats" used for swamp travel. Standard steering systems in use are conventional rudders, variable thrust angles (for water jets) or differential thrust applied to multiple propulsion units. As is true for all emerging scientific endeavor, experimental SES models and testcraft were required to prove candidate designs and conduct basic experiments.

2. The Continuing XR-3 Experiment

In 1965 the XR-3 surface effect ship testcraft was built by the David W. Taylor Model Basin which is now the David W. Taylor Naval Ship Research and Development Center. In the ensuing years it was operated both by the Navy and the Aero-jet General Corporation until 1970 when it was transferred on a permanent basis to the Naval Postgraduate School (NPS), Monterey, California. Since 1970, the XR-3 testcraft has been the

apparatus for a continuing series of experiments involving SES propulsion methods, bow and stern seal dynamics, data acquisition methods, seal loading studies, plenum pressure profiles, maneuvering characteristics, etc. The results have been published in thesis papers by NPS students and reported to the Naval Sea Systems Command (PMS 304).

This series of experiments is continued in this report which examines the horizontal, differential drag forces that are experienced by the bow seal during testcraft turns of various rates conducted while operating at velocities above the hump speed. The term differential drag is used throughout this report and should be taken to mean the total drag experienced by the bow seal of the testcraft as individually measured by the two drag-sensing load cells located equidistant from the centerline of the testcraft in the same (horizontal) plane as the foundation of the bow seal (Fig. 2).

II. POSTULATE

The field of surface effect theory and principles is well established and basically complete with the exception of the interactions occurring at the juncture of the plenum flexible seals and the water surface. Because of the diversity of seal designs and the irregular contours of the water surface, the effort to determine the location and magnitude of the forces acting on these seals has been largely empirical. This report is an addition to the existing body of empirical data and deals specifically with the bow seal differential drag experienced in turns of various rates and various testcraft velocities.

Initially, it is postulated that for any specific velocity there exists a definite relationship between the drag experienced on the port and starboard side of the bow seal and the direction of the turn. Further, it is postulated that this relationship is the same for both right and left turns. Referring to the side of the seal in the direction of the turn as the inboard side, this relationship could be, for example, that the inboard drag is always greater than the outboard drag. The point is to discover the true nature of this relationship of differential drag to the direction of the turn.

It is further postulated that this relationship or pattern of differential drag shows some constant variation with increases in turn rate and testcraft velocity. Proceeding from this bland

postulate, the objective is to empirically discover the nature of the differential drag relationship and its variations.

III. DESCRIPTION OF THE TESTCRAFT XR-3

In the series of studies, experimental results and reports utilizing the XR-3 testcraft, it has been minutely and thoroughly described in references 1, 2, 3 and 6. Notwithstanding, a brief description of the craft should be given to assist readers not familiar with this series of experiments.

A. GENERAL CONSTRUCTION

The XR-3 is a twin hull (sidewall), woodframe and aluminum craft; rectangular in shape, 7.3cm (24 feet) long and 3.65m (3 feet) in height with an all up weight of 2762Kg (6090 pounds).[1] Both sidewall hulls are tapered from a point at the bow to a width of 0.3m at the stern. The inboard surfaces of these two sidewalls are parallel. A horizontal, flat, crossdeck connects the two sidewall hulls from the square bow to a squared stern. The upper side of the crossdeck is called the weather deck and the lower (or underneath) side forms the overhead surface of the plenum chamber and is called the wet deck. The space between these two decks houses air ducting, fuel tanks, engine compartment, data recording instruments and cockpit space. Located between the two sidewalls at the bow is the bow plenum air pressure seal which is attached to the wet deck. This seal

---

[1]All up weight includes all fuel, passengers, instruments, appertances, etc.

(whose lower face is in contact with the water surface) prevents the escape of large amounts of air from the plenum chamber at the bow. Figure 2 shows the general seal construction and attachments. The stern seal, which is similarly configured, accomplishes the same purpose astern. Because this report deals specifically with the bow seal, a detailed description of it and its appendages follows in the next section.

The wet deck, the inboard sidewalls, the two seals and the water surface form a rectangular plenum chamber approximately 6.10m (20 feet) long, 3.05m (16 feet) wide and 0.55m (0.5 foot) high (Fig. 1a).

There are five engine-fan combination units which pressurize the plenum chamber, bow seal and stern seal. The engines are single cylinder, air-cooled, 4-cycle, internal combustion engines; four engines producing 2.5bhp and one producing 5bhp. The fan portions of these units are single stage axial fans which, when driven through a step-up drive/clutch arrangement, deliver air at 1350cufm @ 6.5Psf. Air is delivered to the seals and plenum through a system of tubular metal ducts which are fitted with uni-directional flapper valves and bypass devices which divert excess air from the seals to the plenum as necessary. Two engine-fan units pressurize the plenum, two units pressurize the bow seal and the remaining, larger unit pressurizes the stern seal. Propulsion power for the craft is provided by two 55bhp (@ 5250rpm) Chrysler outboard engines

mounted immediately astern and on the centerline of each sidewall hull. The engines are modified by extended drive shafts to keep the propellers submerged even when the craft is at pressurized height (i.e., "on cushion").

Electrical power is supplied by a self-contained 1500 watt, 110 VAC 60Hz auxiliary power unit, and two 12 VDC storage batteries.

A series of AC-DC and DC-DC converters supply ± 12 VDC and + 28 VDC power to the onboard instrumentation package and ship's service needs as required.

B. BOW SEAL CONSTRUCTION

At the extreme bow of the XR-3, between the two sidewall hulls and attached to the wet deck by four lift sensing devices, is a rectangular, aluminum angle framework to which is attached the flexible bow seal (Fig. 3). There are two drag sensing load cells attached to this framework in the same (horizontal) plane as the framework itself which transmit forward and aft drag data for the seal. The forward face of the flexible seal itself is a gently-curved, spring-stiffened, rectangular planing surface. It is made of rubberized fabric stiffened by 12 equally spaced spring steel stays (approximately 10cm wide by 122cm long) which impart some stiffness to the seal and assist in maintaining seal shape. This planing surface is the only area of water contact on the bow seal. Above the planing surface are two horizontal, tube-shaped compartments (or lobes) of the seal. These compartments cross the width of the seal and the

cross-sectional shape of each tube is that of an elongated tear drop with the "point" toward the bow. The upper lobe is connected to the aluminum framework and the lower lobe. The lower lobe is attached to the reverse (or after) side of the planing surface. The two lobes are vented to one another. The seal's compartments are closed on both ends (adjacent to the sidewalls) by rubberized fabric.

Pressurized air is ducted into the region of the aluminum framework and large holes in the partition between upper and lower compartments permits full inflation of the seal. Although the bow seal pressure can be different from that of the plenum, in most cases, and in this report, it is not significantly different.

C. INSTRUMENTATION

1. Onboard Instrumentation

The XR-3 is instrumented to record, as a function of time, 14 individual variable values simultaneously. The variables of primary interest in this report are as follows:

(1) Bow seal drag
    port (#1)
    starboard (#2)
(2) Velocity
(3) Rudder angle
(4) Turn rate
(5) Pitch angle

(6) Roll angle

(7) Yaw angle

Boland [2] surveys and describes the instrumentation system of the XR-3 in exhaustive and precise detail. For continuity and completeness, the instrumentation apparatus of the bow seal which retrieves the most important data to be analyzed will be described herein.

When in place at the bow of the testcraft, the uppermost surface of the bow seal is the wet deck. Further, the rectangular aluminum framework of the seal is bolted directly to the wet deck. In previous studies an accurate measurement of lift produced by the seal was required and to permit that measurement, the seal construction was modified to its present form. The entire seal was removed from the bow and a 0.635cm aluminum sheet was riveted, glued and sealed to the top of the seal's frame. The covering sheet of aluminum was holed, and upon reinstallation, jointed to the bow seal pressurization vent.

The seal is now a pressurized, separate entity. The seal is attached to and suspended from the wet deck by four lift sensing load cells. These cells are mounted on threaded rods so that the seal may be properly leveled and squared to the wet deck and sidewalls. A small plastic strip on the after portion of the seal attaches to the wet deck and thereby seals the main plenum chamber from air leakage over the bow seal.

The two drag measurement load cells are mounted on the extreme bow of the testcraft in the horizontal plane, one on the port side, the other starboard. They are located equidistant (65.88cm) from the centerline. Aluminum triangular brackets welded to the bow form the fixed support of one end of the load cell. The other end of each cell is attached to the rectangular aluminum frame of the bow seal. This arrangement, which is shown in figure 3, allows the measurement of the differential drag experienced by the bow seal. The four lift measurement cells and the two drag measurement cells are powered by the onboard 12 VDC electrical system through a voltage regulator which reduces the voltage to 5 VDC.

The output of these cells is a ± 5 VDC analog signal which is amplified by a pair of operational amplifiers. Separate lift force and drag force summation circuits are provided to properly add the amplified cell outputs if desired. The resultant load cell analog signals representing individual or total lift or drag are recorded on separate channels of the onboard data recorder, a Pemco 14-channel magnetic tape recorder (Model 120B). The instrumentation circuit is equipped to provide zero or neutral readings and signal inversion where necessary to adhere to the reference measurement system (i.e., positive lift is upward, and positive drag acts in the aft direction).

2. Mobile Data Reduction Facility

As noted above, the data recorder is connected onboard the testcraft for the data collection maneuvers. Upon

completion of the runs, the recorder is installed in a Mobile Data Reduction Facility which is thoroughly described in reference 3. The recorder's magnetic tape is then played back through the data reduction apparatus to produce tangible, time-based recordings of the data collected. It is from these stripchart recordings that the correlation and analysis of variables is performed.

The reduction apparatus consists of a bank of amplifier-filters, a matrix switch selector connecting the 14-channels of recorded information and the nine available amplifier-filters, two 2-channel stripchart recorders and the data recorder. In a typical data reduction sequence, a specific maneuver (classified by testcraft entrance velocity and turn rate executed) is selected to be analyzed. Proper arrangement of the matrix selector would channel four recorded variables to the stripchart pens via the amplifier-filters. The most common selection of variables for this report, for example, was (1) Drag 1, the drag experienced by the port side of the seal, (2) Drag 2, the drag experienced by the starboard side of the seal, (3) $\dot{\psi}$, the testcraft turn rate and (4) V, the testcraft velocity. By observing these variable values for a specific testcraft velocity and turn rate, one point of information was gained about the postulated pattern of differential drag.

IV. DRAG COMPENDIUM

To fully appreciate the material which follows, a brief survey of the specialized meaning of "drag" as applied to surface effect craft is necessary.

A. GENERAL DEFINITION

In the glossary of the respected Jane's Surface Skimmers Hovercraft and Hydrofoils [5], the definition of drag points out its trinary nature.

> "drag-aerodynamic and hydrodynamic resistance encountered by the air cushion vehicle resulting from aerodynamic profile, gain of momentum of air needed for cushion generation, wave making, wetting or skirt contact."

As can be immediately seen, this is a very broad definition and encompasses all the components of drag affecting the entire SES craft. Leaving aside the aerodynamic form drag of the craft and the hydrodynamic drag of the semi-submerged sidewalls, this report deals with the measurement of the components of drag experienced by the seals only, and in particular the flexible bow seal. As pointed out in reference 6, the seal drag is approximately one-third of the total drag experienced by the craft (Fig. 4).

The triple components of bow seal drag are generally catalogued as the drag due to the cushion pressure force, the drag resulting from the aerodynamic shape of the seal, and the hydrodynamic drag resulting from water contact. For purposes of

measurement, only the cushion pressure force and the hydrodynamic force are significant, the aerodynamic drag being orders of magnitude below the other two components. Basically, the aerostatic drag acting on the bow seal is due to the atmospheric overpressure in the plenum chamber. The bow seal is simply a flexible membrane between two regions of differing pressure. Since the overpressure exists in the plenum, it is clear that the seal will feel a force in the forward direction. Since the convention is to measure resistance acting in the aft direction as positive drag, the bow seal will experience a negative drag force due to the plenum overpressure. This negative drag experienced by the bow seal is the dominant drag component until very high testcraft velocities (above approximately 28 knots) are achieved and the aft-acting hydrodynamic drag of the flowing water in contact with the seal exceeds it (Fig. 5).

B. DIFFERENTIAL DRAG

Remembering that the bow seal total drag is then negative for all the velocities of concern here, differential drag can be defined as the simple difference in the drag measured on the right (starboard) side of the seal and that measured on the left (port) side. The "sense" of differential drag will be of importance in dealing with turns to the right and left. The "sense" of differential drag is defined as either positive or negative. A condition of bow seal drag in which the inboard drag value is more positive than the outboard value of drag

is considered positive. Inboard refers to the side of the seal which is located in the direction of the turn. Note that a positive sense of differential drag will imply a clockwise (viewed from above) motion of the bow seal for right turns and a counter-clockwise motion for left turns. This convention was established to conform to the intuitive notion of increased positive drag for the inboard side of the seal. Although clockwise and counter-clockwise motion of the seal is implied, as noted in the description of the bow seal, it is rigidly attached to the testcraft by the six lift and drag sensing cells and no significant motion actually occurs.

V. EXPERIMENTAL PROCEDURE

A. MANEUVERS

Above it was postulated that for a specified testcraft velocity, there is a pattern of differential drag for the direction of turn. There were two types of testcraft maneuvers used in the attempt to uncover this pattern of drag and its variations. In the first type, the "fishook", a constant testcraft velocity was established in a straight line prior to applying a change in directional thrust to the outboard engines. The change in the engine directional thrust was made in a smooth, rapid manner to the desired value and held there until the testcraft completed a 180-degree turn or until required to maneuver for safety. This procedure generated base values of port and starboard drag experienced by the bow seal during the straight portion of the track as well as the values of drag experienced in the turn.

In the second type maneuver, the testcraft was piloted in a path resembling the Spiral of Archimedes. Beginning with the testcraft in a straight constant velocity condition, a slight turn in one direction was established for a brief period. The turn rate was increased in small increments until the maximum turn rate was reached. These runs were conducted for both left and right turning spirals at various velocities.

The essential experimental difference between these two types of runs was in the method of establishing the turn. In the first type, a constant position of the engines was maintained in the hope of establishing a constant turn rate. In the second type turn (the decreasing spiral) the rudder was constantly adjusted to maintain a relatively constant turn rate. Although the two methods would seem to produce the same result, the spiral method was the more satisfactory.

The testcraft conducted several straight runs both before and after each spiral to assist in accurate calibration of the drag sensing cells and to equalize the thrust of the two outboard engines.

B. TEST CONDITIONS

The testcraft's weight was 2762Kg (6090 pounds), all up, and the center of gravity was at its optimum position of 302.26cm (119 inches) forward of the stern on the centerline.

All test maneuvers were conducted at freshwater Lake San Antonio in Monterey County, California. Although the general weather conditions were not considered significant in the testing, it should be noted that the amount of wind and wake generated waves present was the determining factor in the quality of the data recorded.

VI. RESULTS

The pattern of differential drag postulated previously is clearly illustrated by a group of graphs of differential drag versus testcraft velocity with turn rate as a parameter. The construction of these graphs is detailed below as the intermediate work also provides insights into the estimation of differential drag.

A. DATA SELECTION AND INTERMEDIATE WORK

Beginning from the raw data collected in a series of six spiral runs at velocities of 26, 23, 19, 17, 15 and 12 knots (entrance velocity) which is tabulated in Figure 6, the graphs in Figures 7 through 12 were constructed from the stripchart playbacks as described previously. The investigator's choice of where in the analog stripchart playback to select the data representative of the two values of drag which compose differential drag is, inescapably, art. It is clear that the selection of time periods during the turn for which the drag values are estimated is crucial to the resulting pattern. Such phenomena as observable transients, turn rate overshoot due to human error, the general surface condition of the water and the additional disturbances added by the wake of the testcraft (and others) all combine to make the choice of the data point values a matter of sheer, care-filled judgment. In general, the times during which these drag values were estimated from

the analog stripcharts occurred almost immediately after the turn rate was clearly established. These time periods were approximately one minute in duration if possible and the drag (or other) variable values were averaged over this period to a single numerical value. An illustrative sample of the method used and the manner in which this data point decision was made is shown in Figure 13.

These intermediate constructive graphs illustrate that even at this early, rudimentry stage there is some discernable pattern emerging. First, the negative drag experienced by the bow seal increases (i.e, becomes more negative) with increases in turn rate and then decays as turn rate becomes extreme. The second feature of note is that the phenomenon of differential drag does not begin to appear until the testcraft reaches a velocity in the neighborhood of 17 knots. Below this velocity there may be differential drag, but it is smaller than the experimental error that is encountered with the present load measurement apparatus. This onset of differential drag is characterized by large differences in port and starboard drag values and intersections of the port and starboard drag curves. The final and perhaps most notable characteristic of these intermediate graphs is that when differential drag does appear, the negative drag on the bow seal is greatest on the outboard side of the seal, i.e., the side away from the direction of the turn. Since the testcraft normally does roll slightly inboard in a turn, this characteristic supports the

intuitive notion that a force couple would be present on the seal which acts clockwise in right turns and counter-clockwise in left turns of substantial rates and significant velocities.

Leaving this first set of intermediate graphs for the moment, additional data was extracted from the analog playback stripcharts highlighting the relationship between the testcraft velocity degradation experienced in the turns and the associated turn rate at that moment. This data was extracted for both right and left turns in the same manner described above and is noted in Figure 14. Plotting this data results in the six graphs of turn rate versus velocity (Fig. 15) for right turns and six similar graphs for left turns (Fig. 16). This set of graphs is now the second set of intermediate constructive graphs prepared to yield the desired product. Rates of turn (left and right) from one to eight degrees per second are now selected as the parameter for the eight final graphs of differential drag versus testcraft velocity for a constant turn rate. For each value of turn rate, the velocities experienced were taken from the curves in the second intermediate set. Also for the same turn rate, the corresponding values of port and starboard drag were taken from the first set of intermediate graphs. This agglomerated data is tabulated in Figure 17 for right turns and Figure 18 for left turns. The desired constant turn rate graphs were produced from these two data fields and are shown in Figures 19 through 31. They also display definite patterns and interesting characteristics.

B. SUMMARY GRAPHS

The most pronounced feature of these graphs for both right and left turns is the steepness of the curves. The increase of positive drag on both sides of the seal with an increase in velocity is large in most parts of the curve. The regions which are enclosed by, or lie between, the two lines of port and starboard drag on each group represent the differential drag experienced by the bow seal for a constant rate turn at various testcraft velocities. As testcraft velocity increases for a constant turn rate, the "sense" of the differential drag reverses at the intersections of the two lines of drag. Also note that above a turn rate of six degrees per second for right turns and five degrees per second for left turns, there are no intersections at any velocity indicating that the drag is always greater on the inboard side of the seal, the side in the direction of the turn. The "sense" of this drag simply refers to the location of the resultant force on the seal, either the outboard side, or the inboard side, and its direction (either forward or aft).

To assist in picturing these combinations of location and direction of the resultant bow seal differential drag forces, two composite, summary graphs of differential drag versus velocity for various rates of turn, both right and left, were obtained from the constant turn rate graphs (Fig. 19 through 31) using the data tabulated in Figure 32. The composite, summary graphs are shown in Figures 33 and 34. The convention

used in plotting these graphs is that the differential drag is positive if the resultant drag on the seal is positive on the inboard side of the seal, and negative if the resultant drag is positive on the outboard side of the seal, exactly as noted in Section IV. This convention is further illustrated in Figures 35 and 36.

These two summary graphs show most clearly the patterns of differential drag that have been sought. Figure 33 for the right turns shows almost two separate patterns of drag, one for low turn rates of one to four degrees per second and another for higher turn rates of five to eight degrees per second. Broadly speaking, for the lower turn rates, the starboard negative drag is less than (or more positive than) the drag on the port side of the seal. The unusual aspect here is that this arrangement of drag forces produces a horizontal torque on the seal which is in the opposite direction of the turn. For a low speed, low right turn rate maneuver, the bow seal attempts to "turn" left. However, as the testcraft velocity increases above approximately 21 knots, even for low right turn rates, the differential drag goes positive and the intuitive positive-inboard drag situation exists. The high right turn rate pattern of differential drag is as expected showing the bow seal experiencing an increasing positive drag on the starboard (inboard) side as the velocity increases. But there is a definite decline in negative drag as the testcraft enters the higher velocities above 18 knots.

Although the same spiral turn maneuvers were made in both right and left directions, the testcraft showed a distinct tendency to come "off cushion" earlier in the left hand turns than in the right. As a result the data for the left turns is not as extensive as that for the right. Figure 34 shows that for left turns, only the relatively low turn rate data can be observed. Notwithstanding, it is interesting to note that this data shows an exactly opposite tendency for the seal than does the right turn data. Generally, the seal experiences positive differential drag for low turn rates until the high velocities are reached. That means that as the testcraft turns left at a low rate and velocity, the seal also attempts to "turn" left, in precise opposition to the result noted for the similar right turns.

The effects of testcraft roll and pitch on the patterns of differential drag observed were not determined quantitatively as a careful review of the available data collected showed that measurable fluctuations, correlative with changes in turn rate and velocity did not occur.

VII. CONCLUSIONS

With respect to the postulate set forth in Section II, from the evidence gathered and the results obtained, it is clear that there is a definite relationship between differential drag and the direction of the turn. However, contrary to the claim of the postulate, this relationship is not the same for left and right turns. The relationship for right turns is consistent and clear; that for left turns is weak, contradictory and opposed to the relationship evidenced in the right turns. As for the variation previously asserted, it is comforting that differential drag does at least appear to have its onset in the same general manner for turns in both directions and that its variations are similar for increases in turn rate and velocity.

A possible explanation of the anomalies in the right and left turns might lie in

a. The normal forces produced by non-counter-rotating propellers.

b. The steering system currently employed wherein the port engine is directly steered and the starboard engine follows. Due to the linkage arrangement, the two engines do not trail at exactly the same angle and may introduce differential thrusting effects.

As velocity decreases in a turn (Fig. 35 is typical) the "negative" drag increases to a maximum value and then decreases.

This means that the hydro forces, i.e., hydrodynamic and hydrostatic forces, decrease as velocity is lost in the turn (as would be expected) until the bow seal is returned to Hump conditions. Below this velocity, the hydro forces once again increase. At low values of turn rate (Fig. 33 is typical) the general "sense" of the bow seal drag is positive, i.e., higher drag occurs on the inside of the seal. As the turn rate decreases, there is a reversal of this "sense". At the higher velocities with low turn rates, e.g., below four degrees per second and above 19 knots, there is effectively no differential in the drag components.

VIII. RECOMMENDATIONS

1. Conduct experiments with lateral bow seal deflection control (pull up on the seal on one side in a turn) to ascertain the effects of this type of control.

2. Conduct experiments with the drag cells located further apart to emphasize the differentials.

3. Repeat the experiments of this report with a bow seal more similar to that proposed for the 3K-SES (a small bag with planing surfaces, rather than the planing surfaces as a part of the bag).

4. Devise a method to exclude the aerostatic forces from the measurements as in the NSRDC experiments by Heber [4]. This would tend to eliminate the "negative drag" confusion.

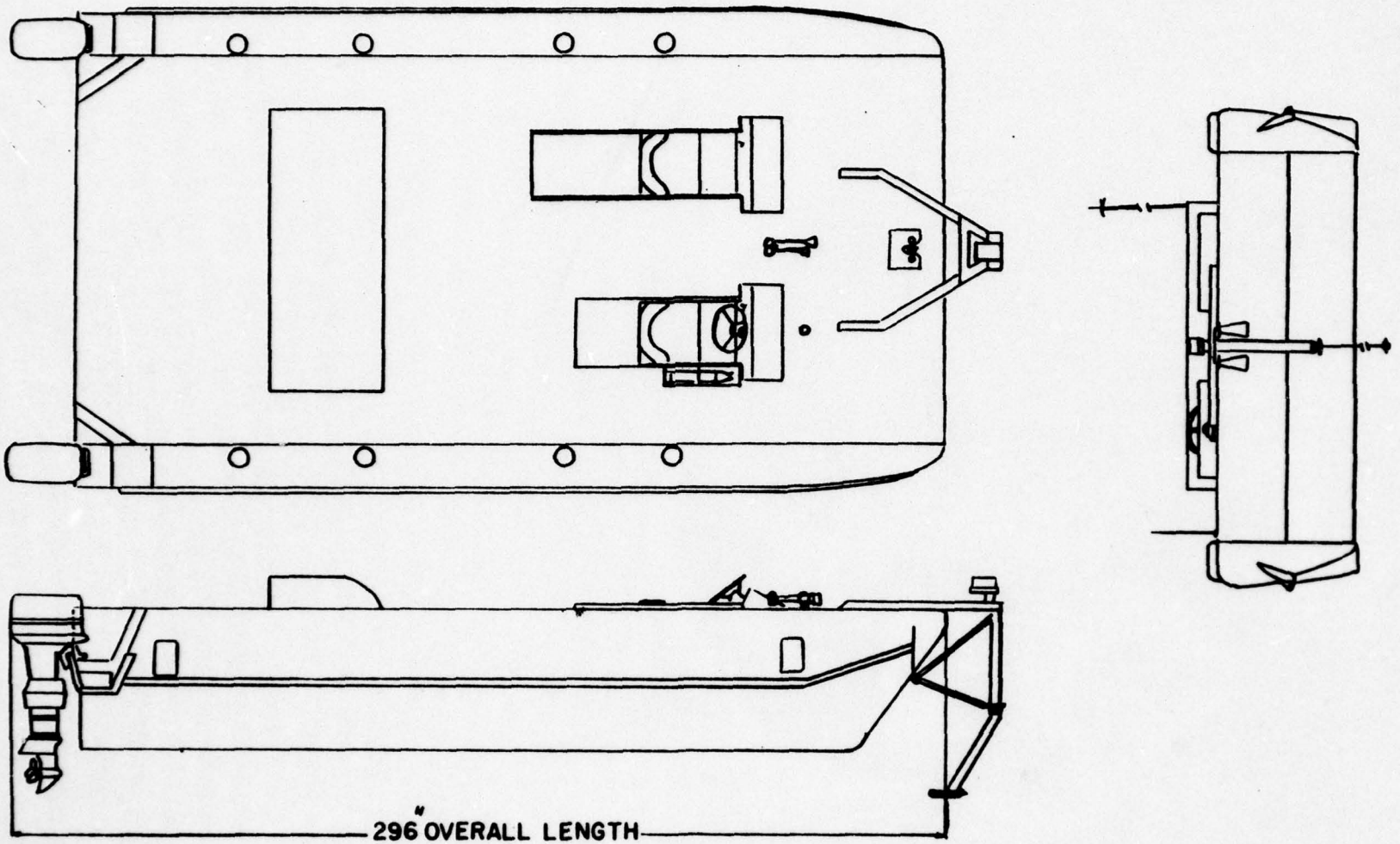

Figure 1

XR-3 Schematic

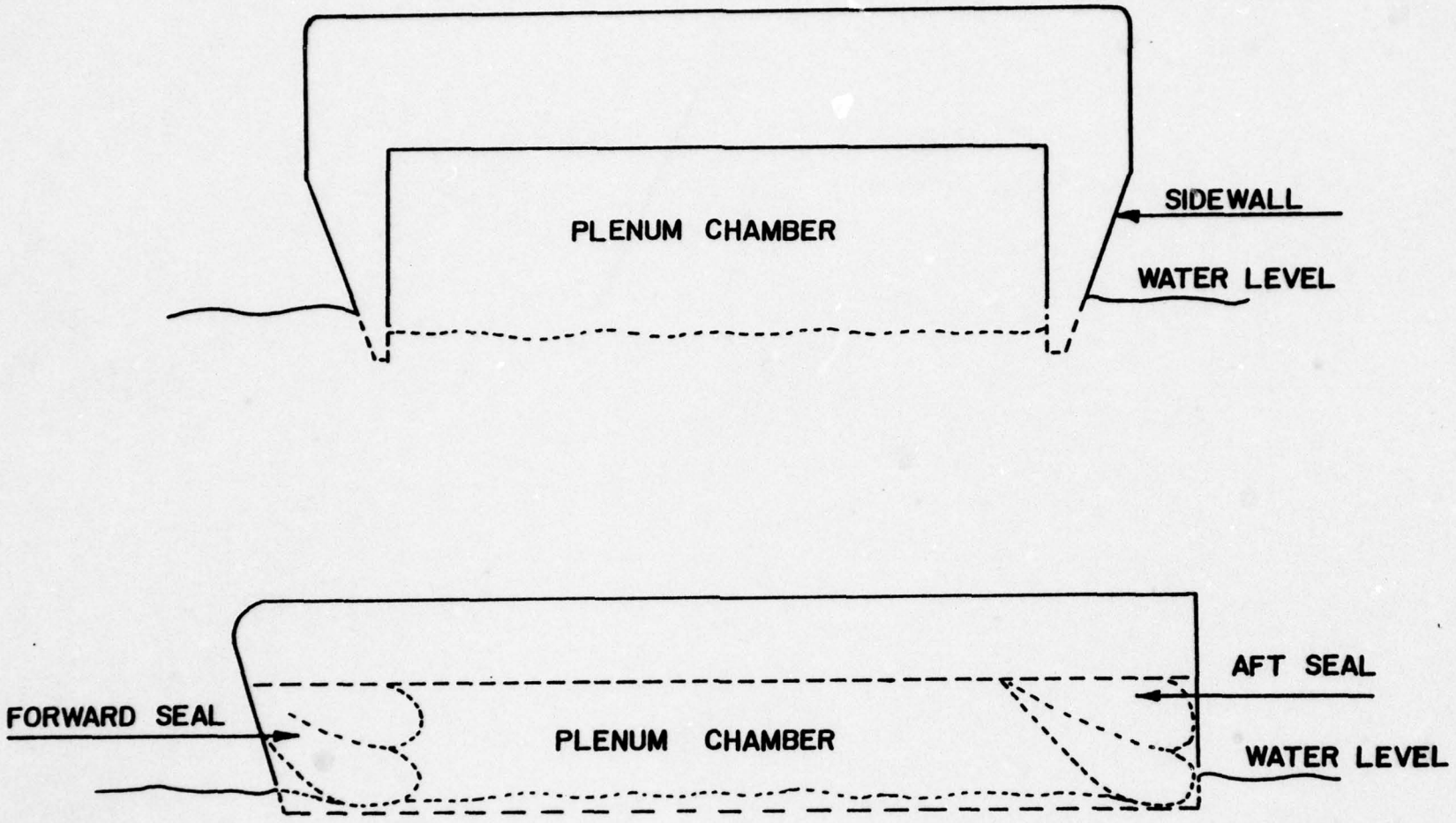

Figure 1a

Plenum Chamber Outline

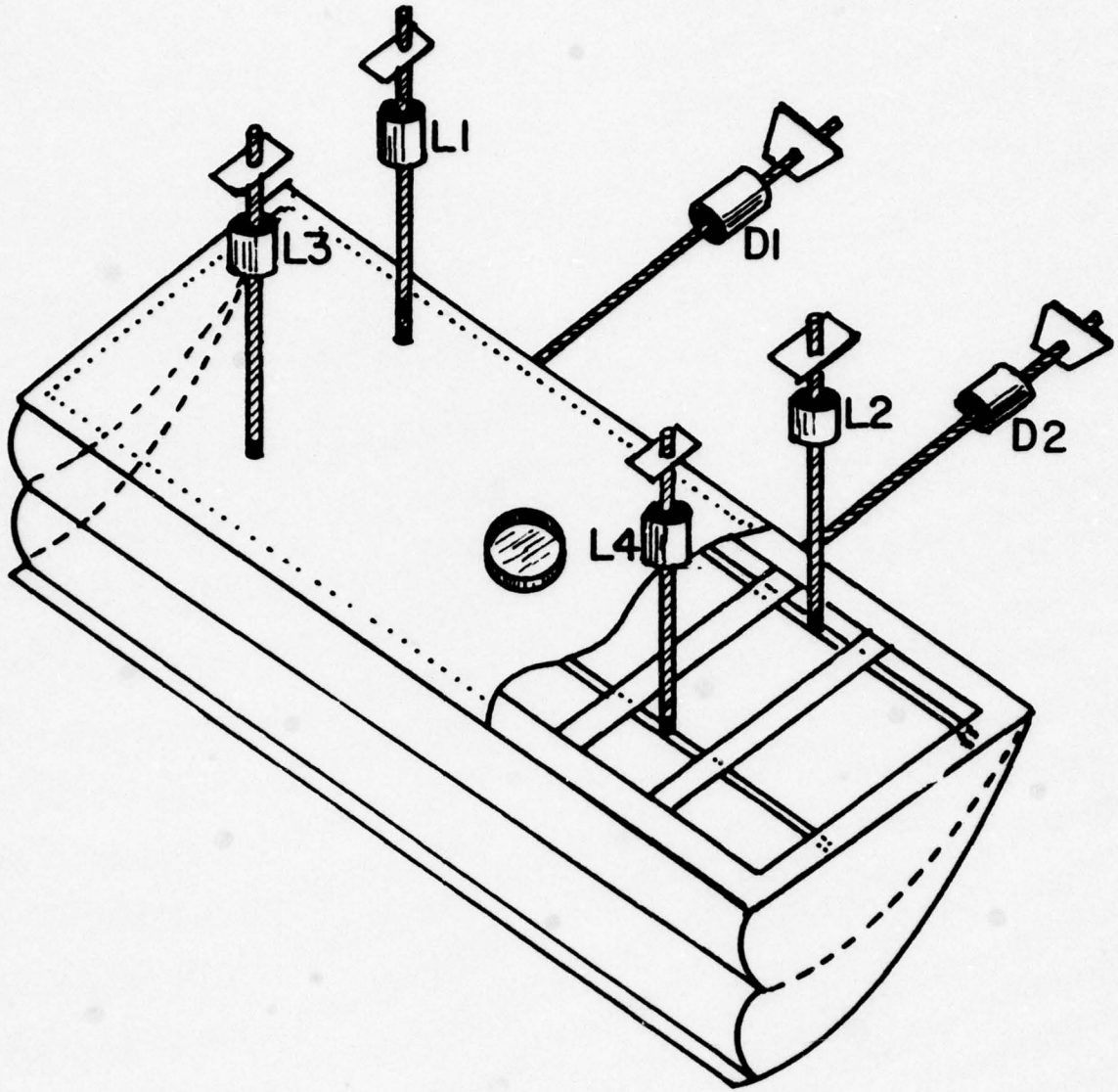

Figure 2

Bow Seal Showing Lift and Drag Cells

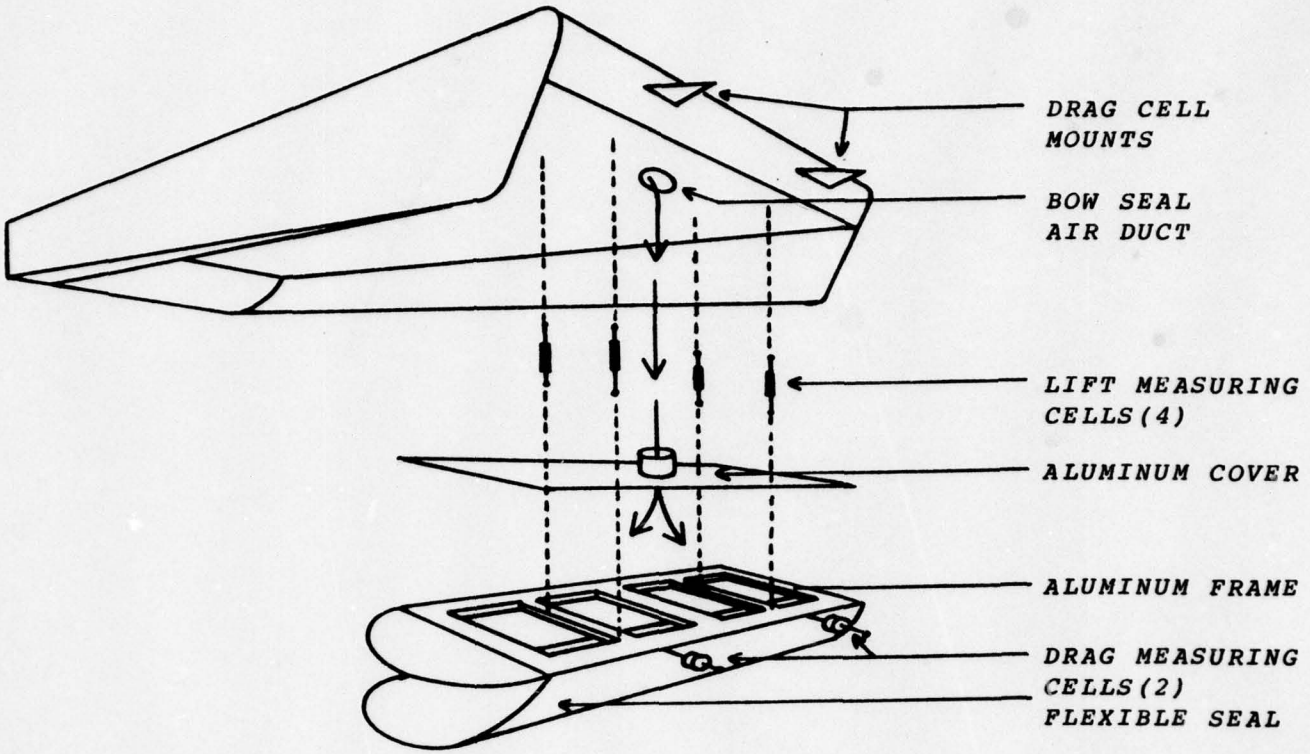

Figure 3

XR-3 Bow Seal Placement and Construction

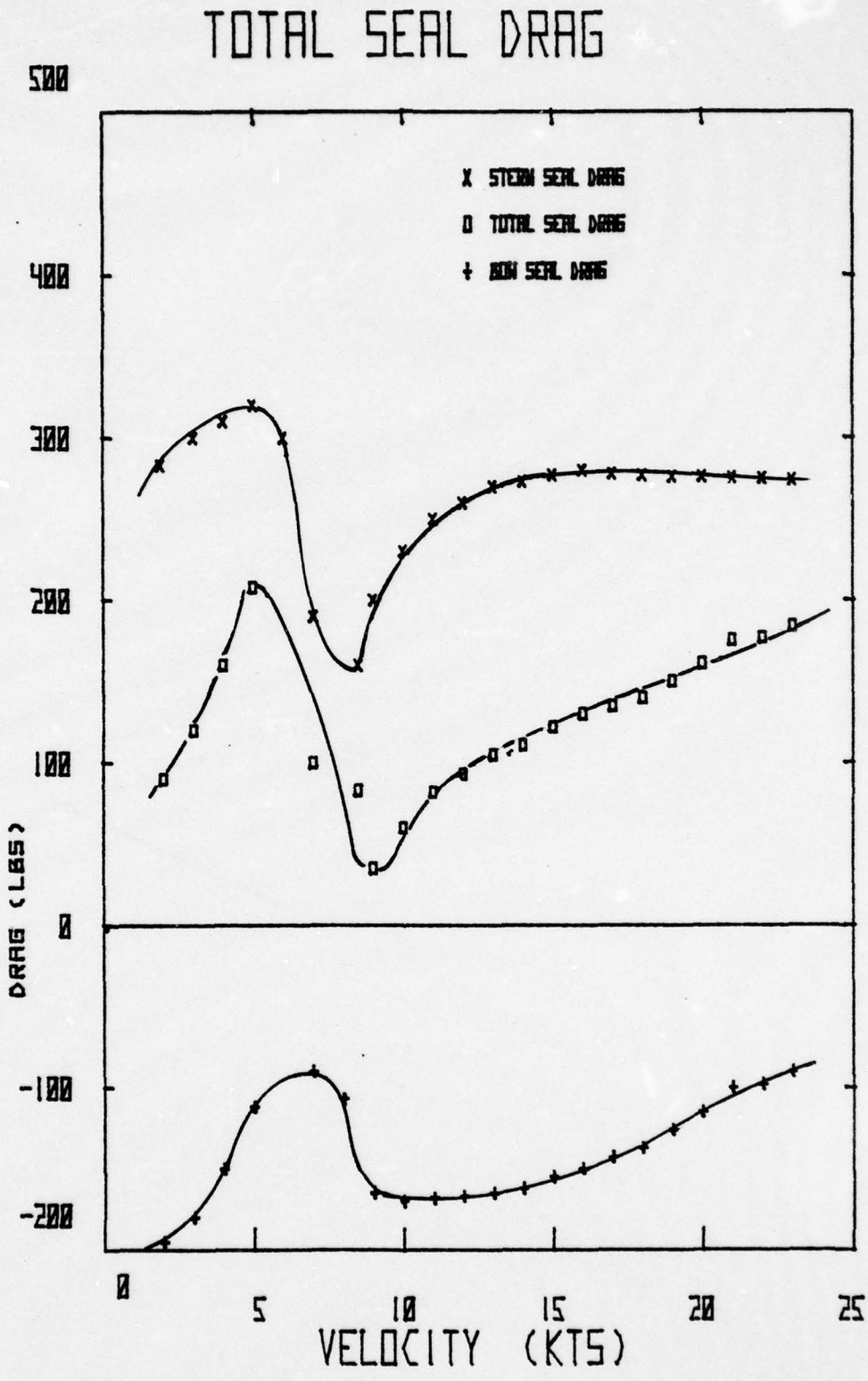

Figure 4

Total Seal Drag

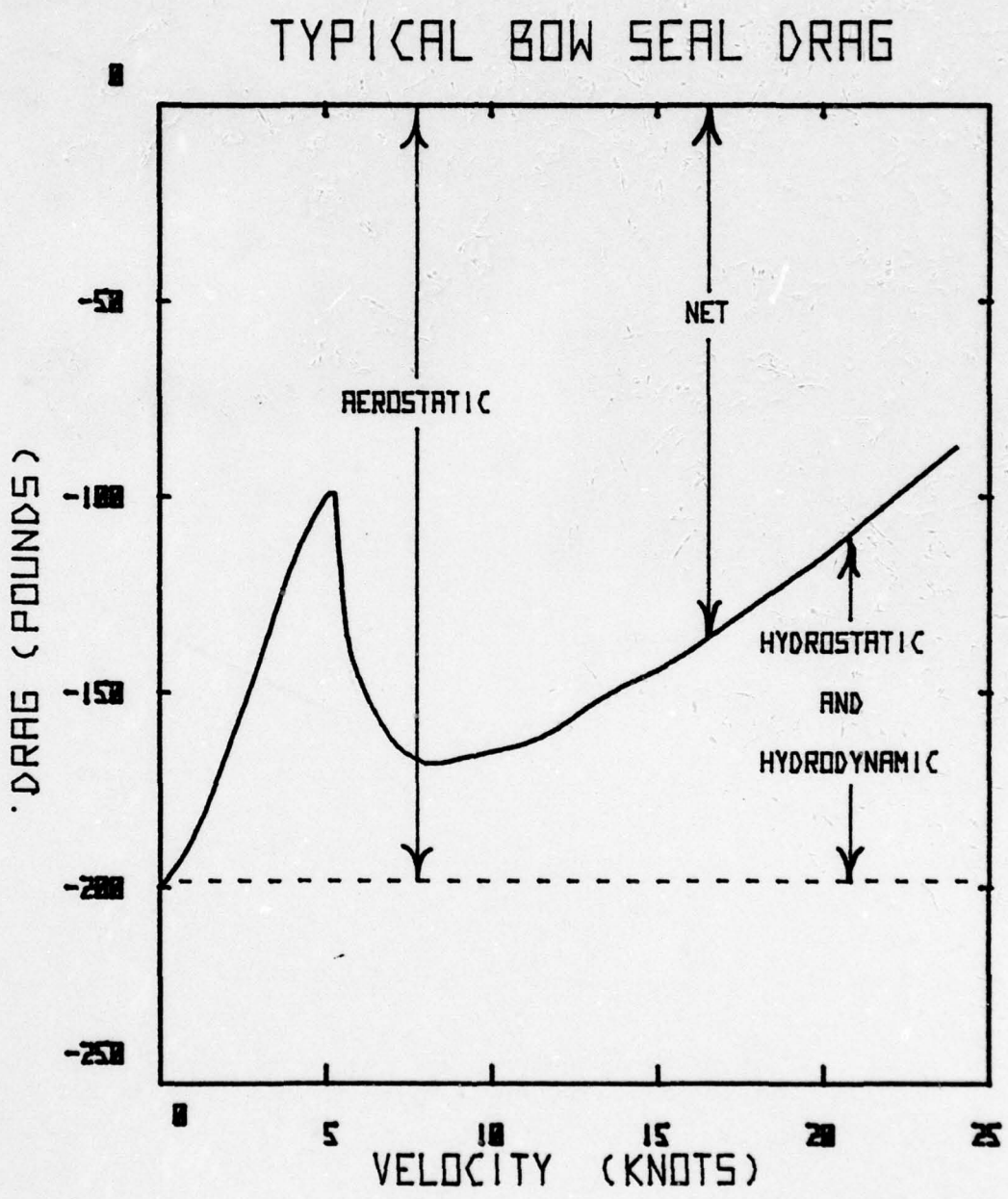

Figure 5

Typical Bow Seal Drag

Figure 6

Data Table (Intermediate Group)

Entrance Speed (kts)	Turn Rate (degrees per sec.)	Port Drag (negative pounds)	Stbd. Drag (negative pounds)
26	S & L	85	88
	R 2.0	97	97
	R 4.1	107	103
	R 5.8	120	103
	R 6.8	127	102
	R 8.8	130	105
	R 10+	145	90
26	S & L	87	87
	L 0.3	90	88
	L 1.7	96	94
	L 2.3	102	98
	L 4.3	102	100
	L 6.0	100	115
	L 7.6	99	122
23	S & L	85	88
	R 1.1	90	90
	R 2.6	101	99
	R 4.4	114	115
	R 6.6	143	108
	R 9.0	140	95
23	S & L	93	93
	L 1.1	98	98
	L 3.0	110	110
	L 5.2	115	117
	L 7.2	115	125

Figure 6 (cont.)

Entrance Speed (kts)	Turn Rate (degrees per sec.)	Port Drag (negative pounds)	Stbd. Drag (negative pounds)
19	S & L	106	126
	R 1.1	110	131
	R 3.5	127	145
	R 6.5	150	150
	R 8.8	155	145
19	S & L	120	125
	L 1.0	124	123
	L 1.7	124	127
	L 3.4	127	130
	L 4.9	141	145
17	S & L	115	130
	R 2.0	123	133
	R 3.8	133	150
	R 5.4	150	140
17	L 0.1	135	138
	L 1.9	136	139
	L 3.0	134	140
	L 4.3	141	150
15	S & L	120	128
	R 1.4	126	134
	R 2.2	128	133
	R 3.4	130	139
15	S & L	137	138
	L 0.2	137	140
	L 1.1	138	141
	L 2.0	139	141
	L 3.3	135	138
12	S & L	130	125
	R 1.4	133	127
	R 3.2	134	129
	R 4.0	136	132

Figure 6 (cont.)

Entrance Speed (kts)	Turn Rate (degrees per sec.)	Port Drag (negative pounds)	Stbd. Drag (negative pounds)
12	L 0.6	132	124
	L 1.6	129	125
	L 2.7	127	124

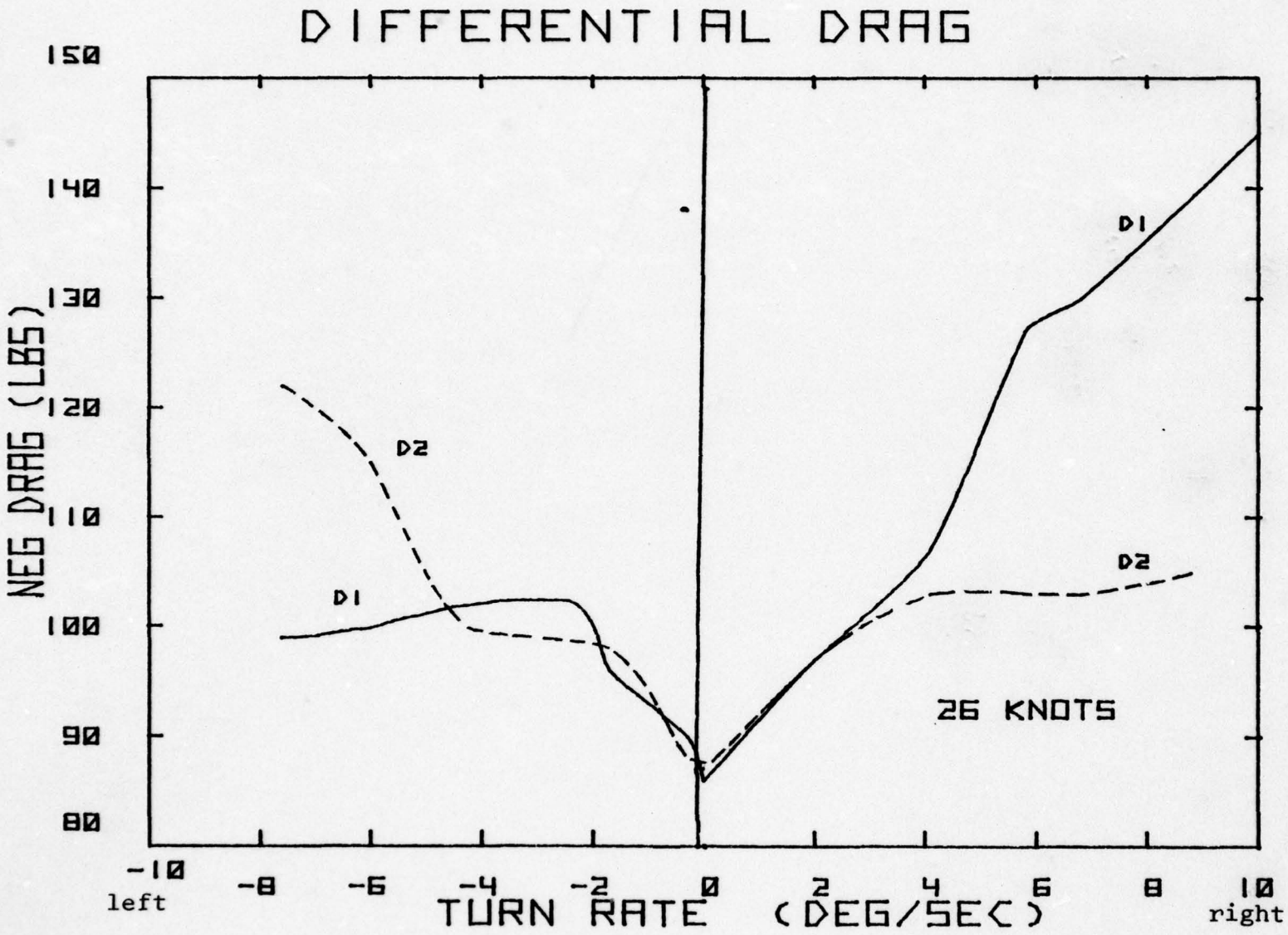

Figure 7

Differential Drag versus Turn Rate - 26 knots

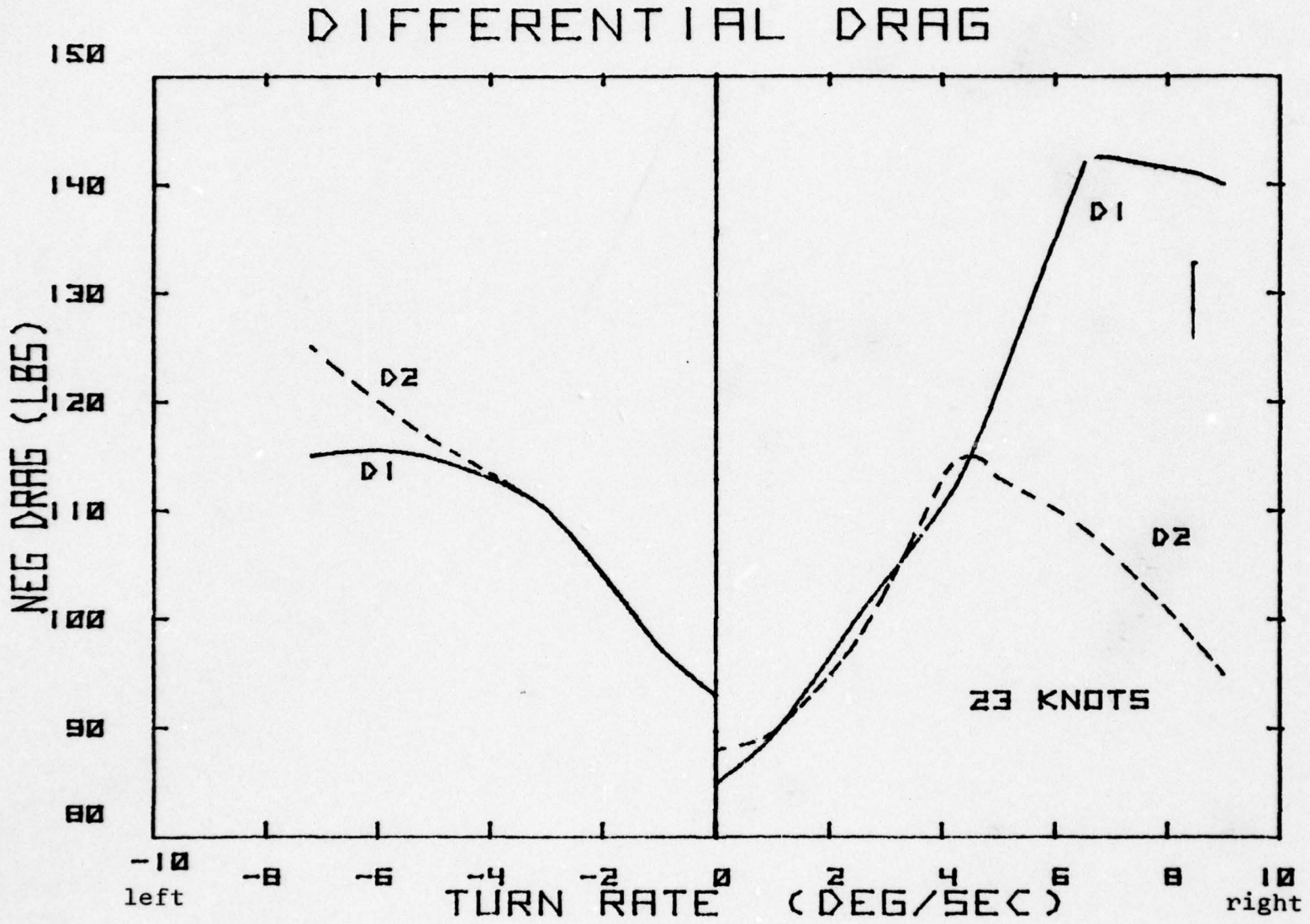

Figure 8

Differential Drag versus Turn Rate - 23 knots

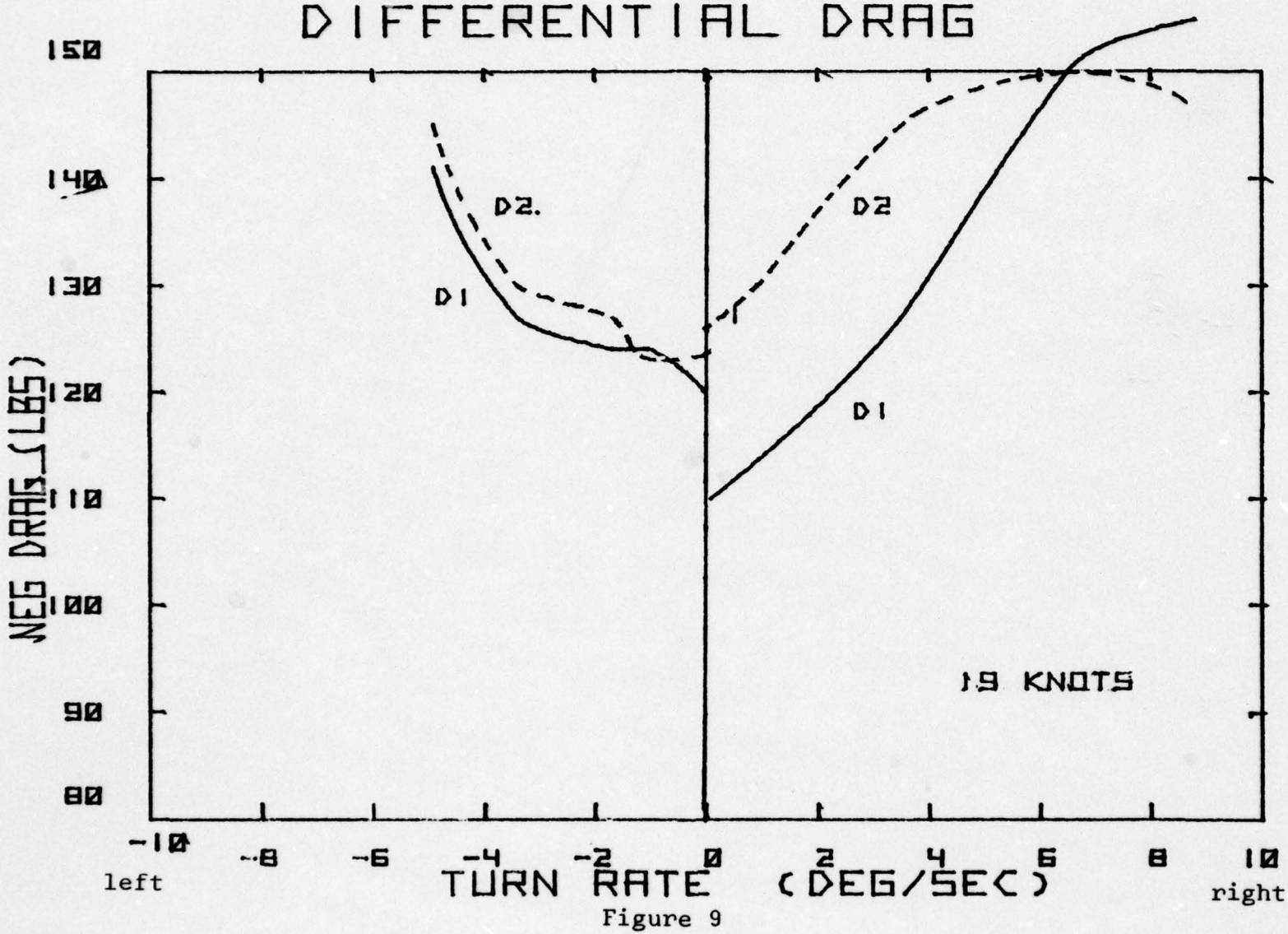

Figure 9

Differential Drag versus Turn Rate - 19 knots

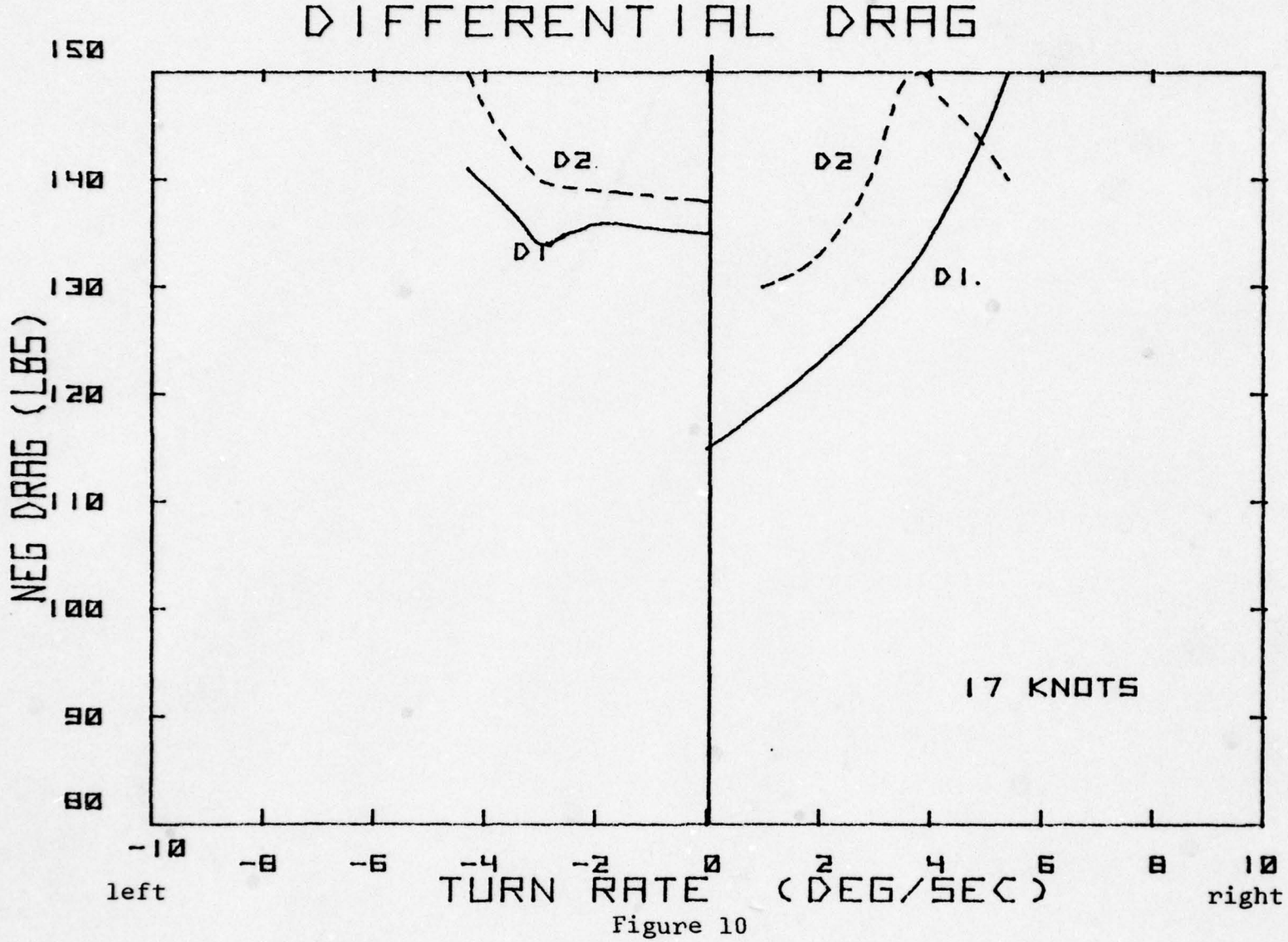

Figure 10

Differential Drag versus Turn Rate - 17 knots

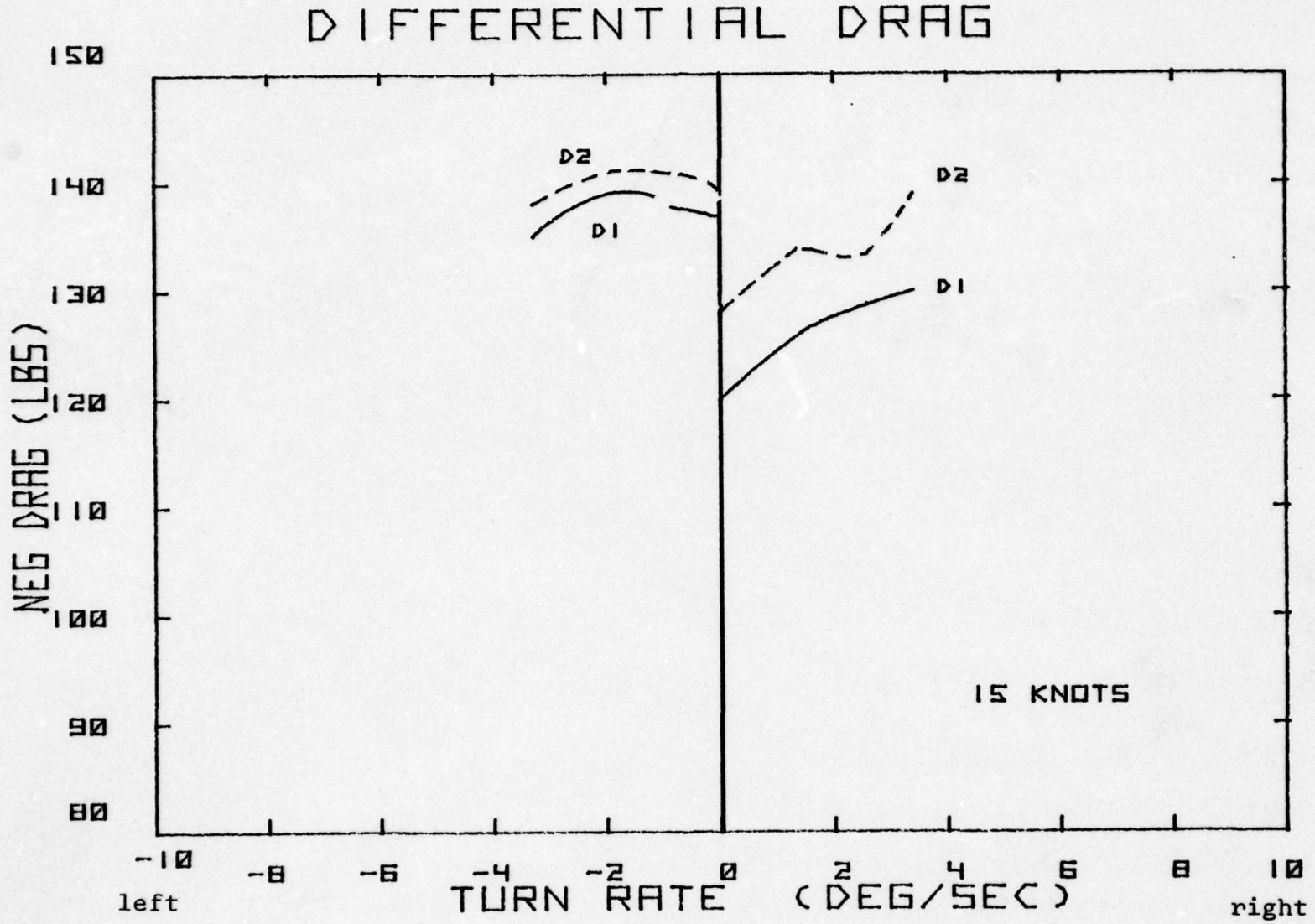

Figure 11

Differential Drag versus Turn Rate - 15 knots

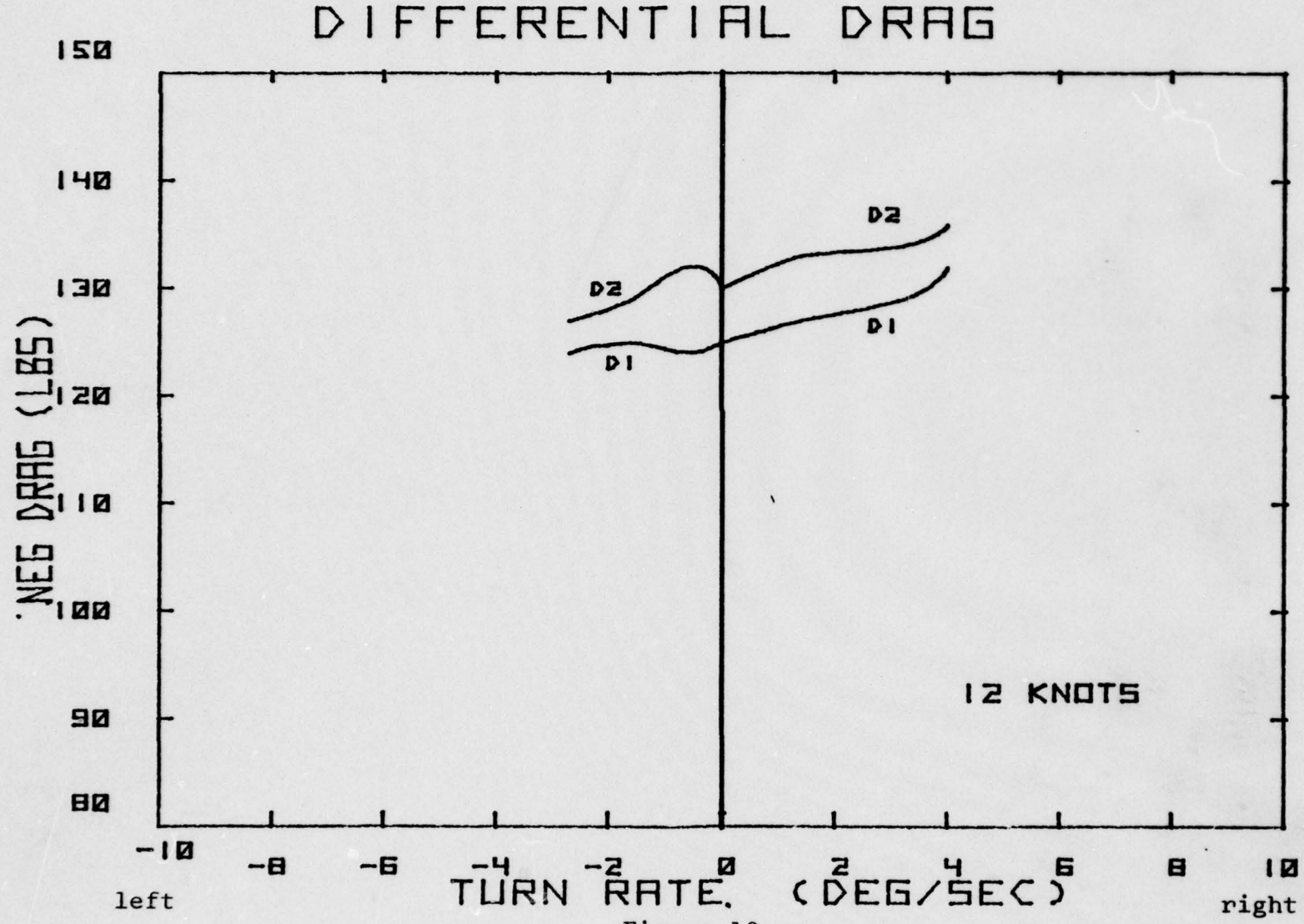

Figure 12

Differential Draf versus Turn Rate - 12 knots

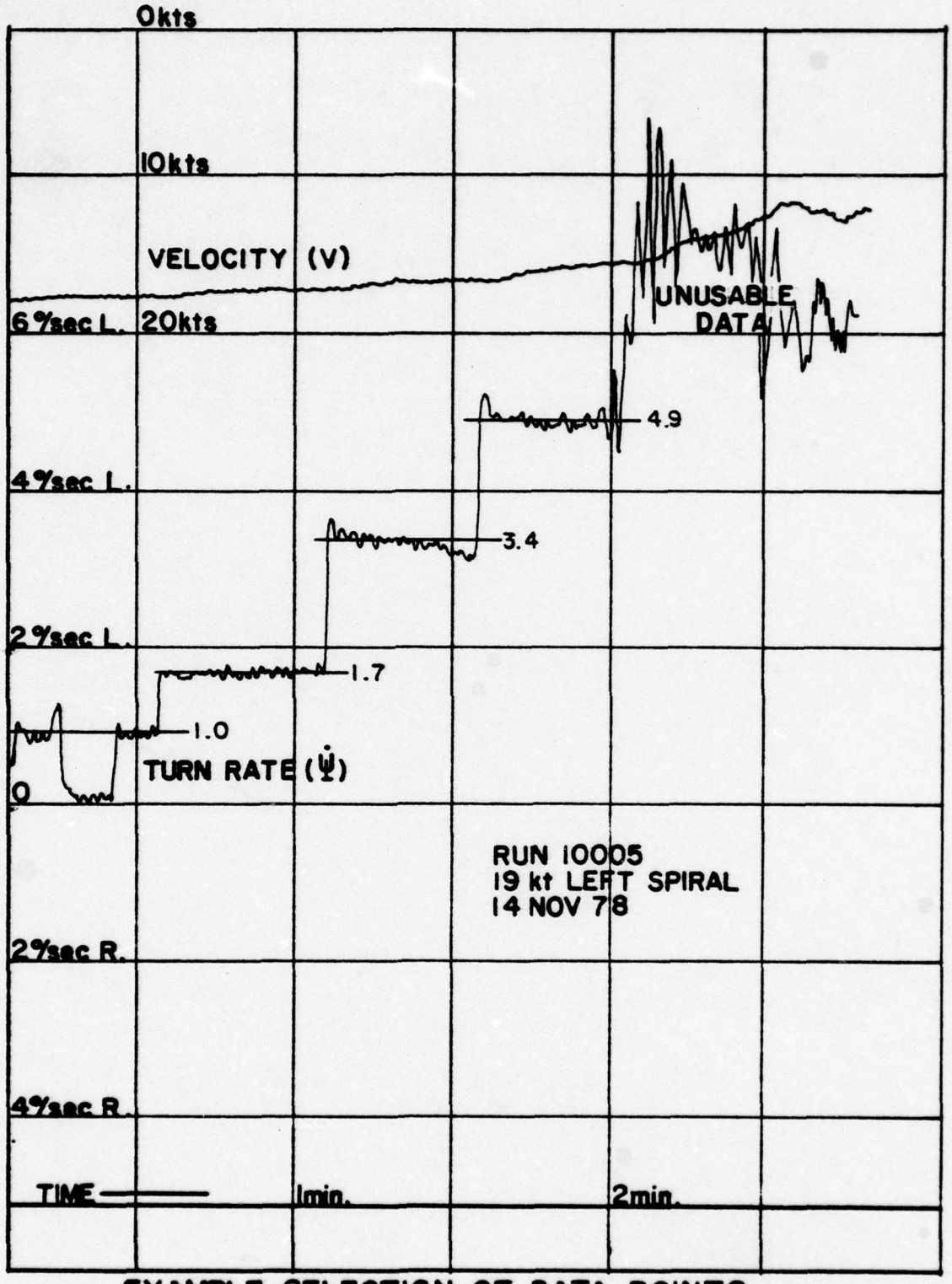

Figure 13

Example Selection of Data Points

Figure 14

Velocity Degradation Data Table

Entrance Speed (kts)	Right Turn Rate (deg/sec.)	Velocity (kts)	Left Turn Rate (deg/sec)	Velocity (kts)
26	2.0	27.0	0.3	25.5
	4.1	26.0	1.7	25.0
	5.8	25.5	2.3	23.5
	6.6	25.0	4.3	23.5
	8.8	24.5	6.0	22.5
			7.6	22.0
			9.2	21.0
23	1.1	23.0	1.1	22.5
	2.6	22.3	3.0	21.5
	4.4	22.0	5.2	20.5
	6.6	20.5	7.2	19.5
	9.0	19.0		
19	1.1	18.0	1.0	18.0
	3.5	16.5	1.7	17.0
	6.5	15.0	3.4	16.5
	8.8	13.5	4.9	15.5
17	2.0	18.0	0.1	17.5
	3.8	17.0	1.9	16.5
	5.4	15.0	3.0	16.0
			4.3	14.0
15	1.4	15.0	0.2	15.0
	2.2	14.0	1.1	14.5
	3.4	13.0	2.0	14.0
	5.2	12.0	3.3	12.5
12	1.4	12.5	0.6	12.5
	3.2	11.5	1.6	12.5
	4.0	11.0	2.7	11.5

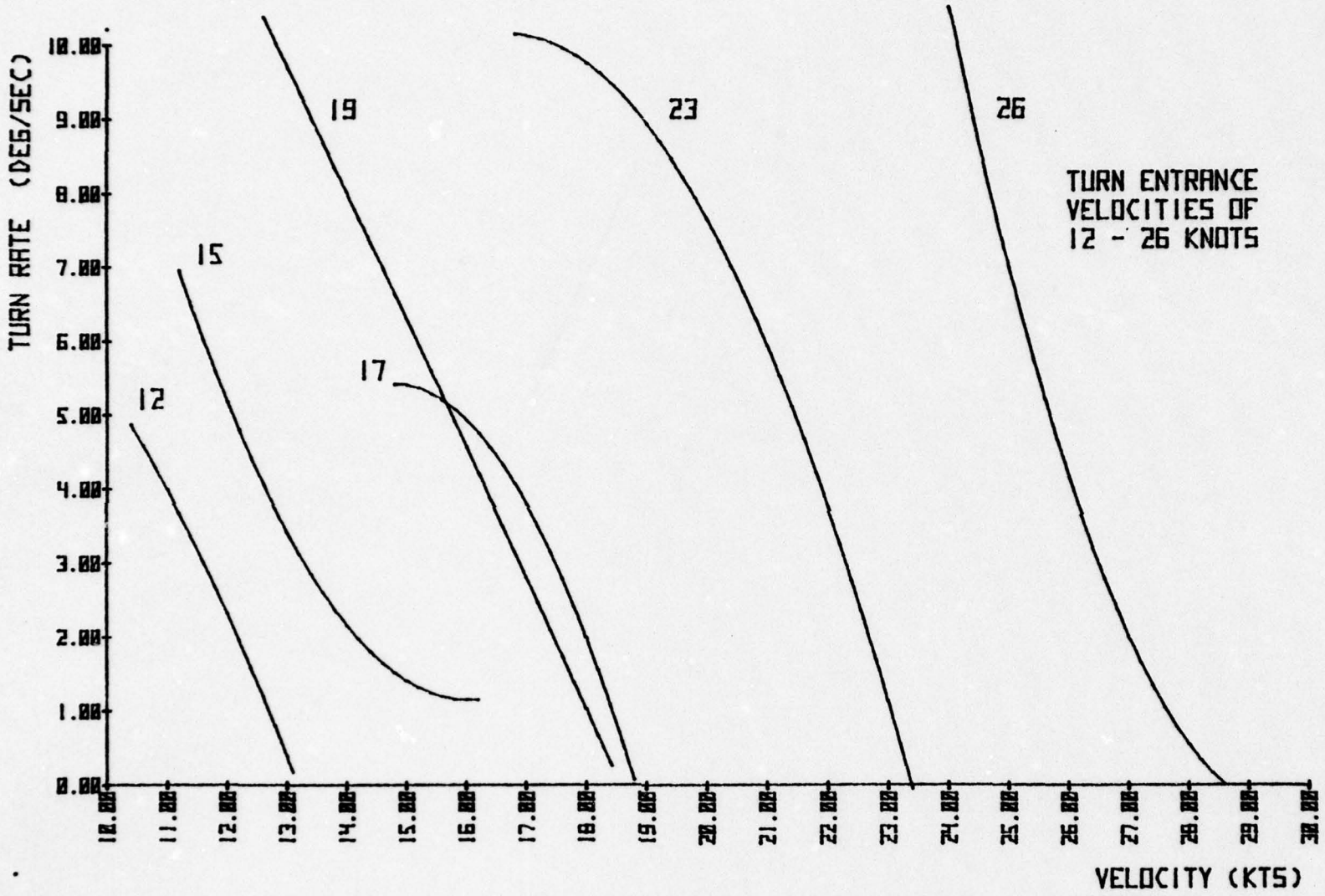

VELOCITY DEGRADATION FOR RIGHT TURNS

Figure 15

Velocity Degradation for Right Turns

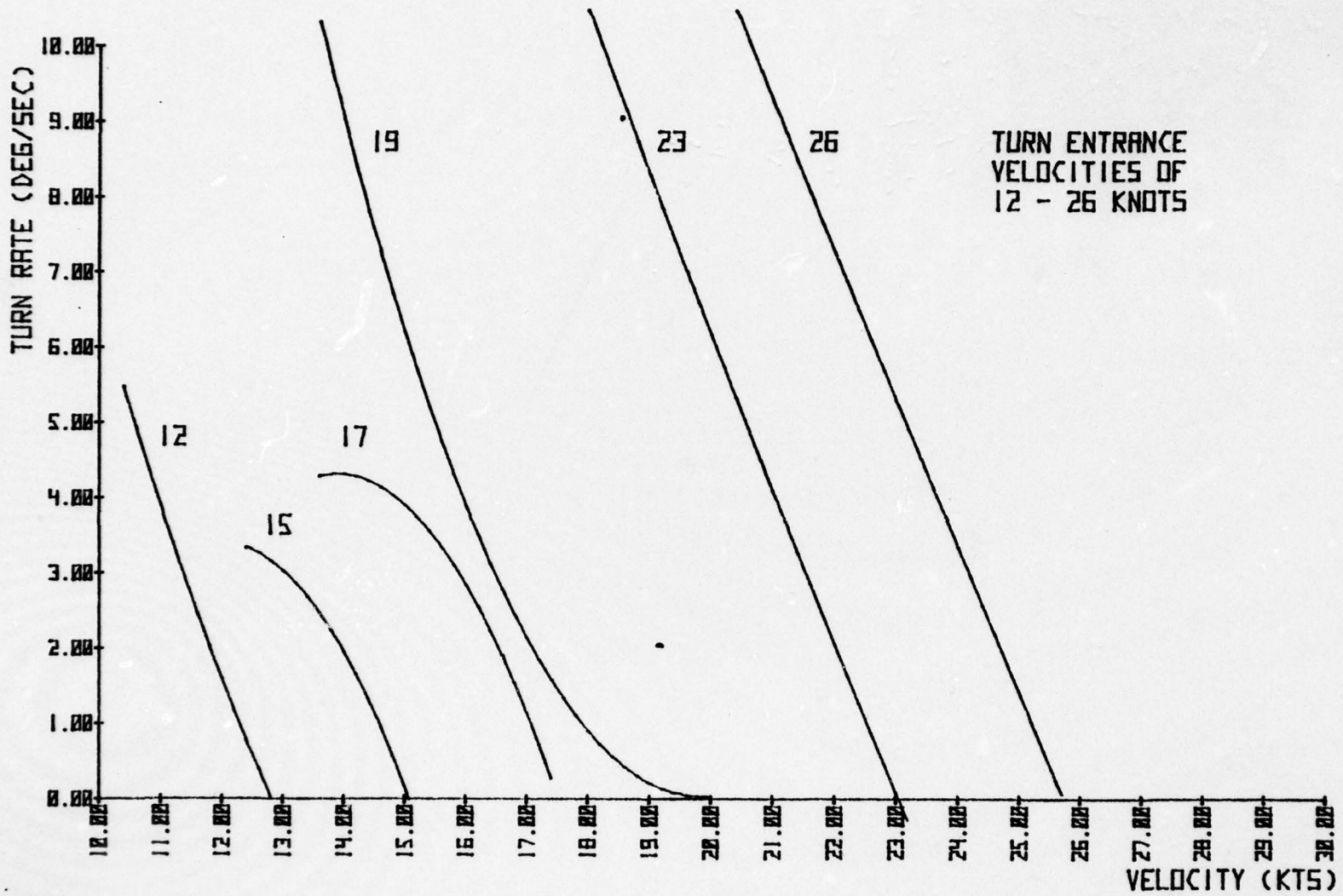

VELOCITY DEGRADATION FOR LEFT TURNS

Figure 16

Velocity Degradation for Left Turns

Figure 17

Right Turn Drag versus Velocity Data Table

Turn Rate (deg/sec)	Turn Entrance Speed (kts) 26		23		19		17		15		12	
1R	27.8	93.0 92.0	23.0	89.0 90.0	18.0	110.0 130.0	18.4	118.0 131.0	15.6	124.0 133.0	12.8	132.0 126.0
2R	27.0	97.0 97.0	22.4	96.0 93.0	17.4	113.0 137.0	18.0	123.0 133.0	14.3	128.0 133.0	12.2	134.0 128.0
3R	26.5	102.0 100.0	22.0	104.0 102.0	16.6	122.0 144.0	17.5	128.0 142.0	13.3	130.0 136.0	11.6	134.0 129.0
4R	26.0	107.0 103.0	21.8	111.0 115.0	16.2	132.0 147.0	16.7	134.0 150.0	12.6	131.0 -	11.0	136.0 132.0
5R	25.7	113.0 103.0	21.5	126.0 114.0	15.6	141.0 149.0	15.6	144.0 144.0	12.0	- -	10.2	- -
6R	25.4	120.0 103.0	20.8	142.0 110.0	15.1	147.0 150.0	14.5	- -	11.7	- -	-	- -
7R	24.9	127.0 102.0	20.3	143.0 106.0	14.6	152.0 150.0	-	- -	-	- -	-	- -
8R	24.6	128.0 103.0	19.5	142.0 101.0	13.9	154.0 148.0	-	- -	-	- -	-	- -
9R	24.4	130.0 105.0	19.0	140.0 95.0	13.4	155.0 144.0	-	- -	-	- -	-	- -

_____ Extrapolated Values

Key: Velocity (kts) Port Drag (neg lbs) Stbd Drag (neg lbs)

Figure 18

Left Turn Drag versus Velocity Data Table

Turn Rate (deg/sec)	Turn Entrance Speed (kts) 26		23		19		17		15		12	
1	25.3	93.0 91.0	22.5	98.0 9810	18.3	124.0 122.0	17.0	136.0 139.0	14.5	138.0 141.0	12.8	131.0 125.0
2	24.8	99.0 97.0	22.0	103.0 103.0	17.0	124.0 128.0	16.5	136.0 139.0	14.0	138.0 141.0	12.0	128.0 124.0
3	24.0	104.0 99.0	21.5	110.0 110.0	16.5	126.0 129.0	16.0	134.0 140.0	13.0	134.0 138.0	11.3	126.0 123.0
4	23.5	103.0 100.0	21.0	113.0 114.0	16.0	131.0 135.0	14.5	138.0 148.0	12.3	- -	-	- -
5	23.0	101.0 106.0	20.8	115.0 117.0	15.3	141.0 145.0	13.5	- -	-	- -	-	- -
6	22.5	100.0 115.0	20.0	115.0 120.0	-	- -	-	- -	-	- -	-	- -
7	22.5	99.0 118.0	19.5	115.0 124.0	-	- -	-	- -	-	- -	-	- -
8	21.8	99.0 124.0	19.0	- -	-	- -	-	- -	-	- -	-	- -
9	21.5	- -	18.5	- -	-	- -	-	- -	-	- -	-	- -

____Extrapolated Data

Key: Velocity (kts) Port Drag (neg lbs) Stbd Drag (neg lbs)

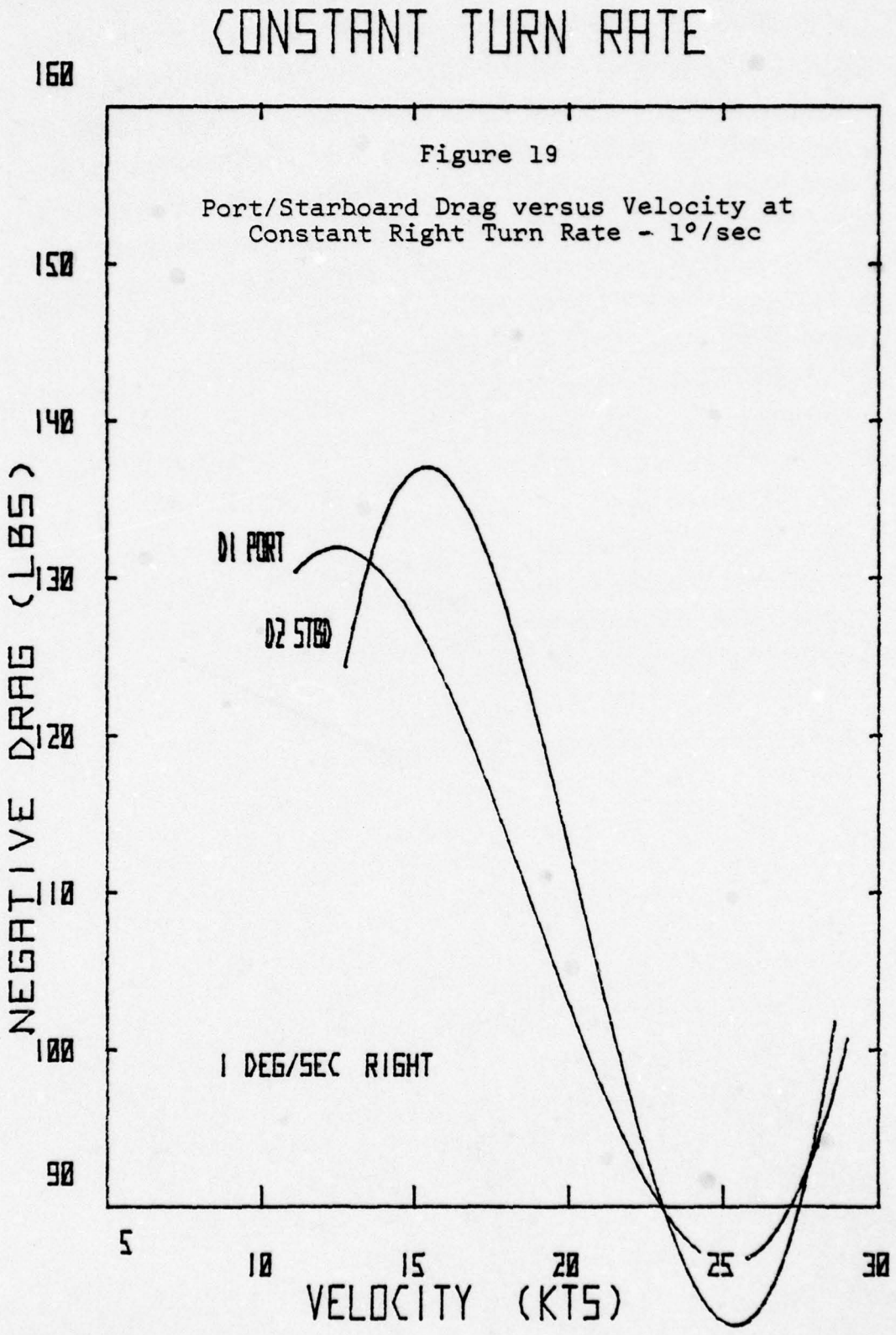

Figure 19

Port/Starboard Drag versus Velocity at Constant Right Turn Rate - 1°/sec

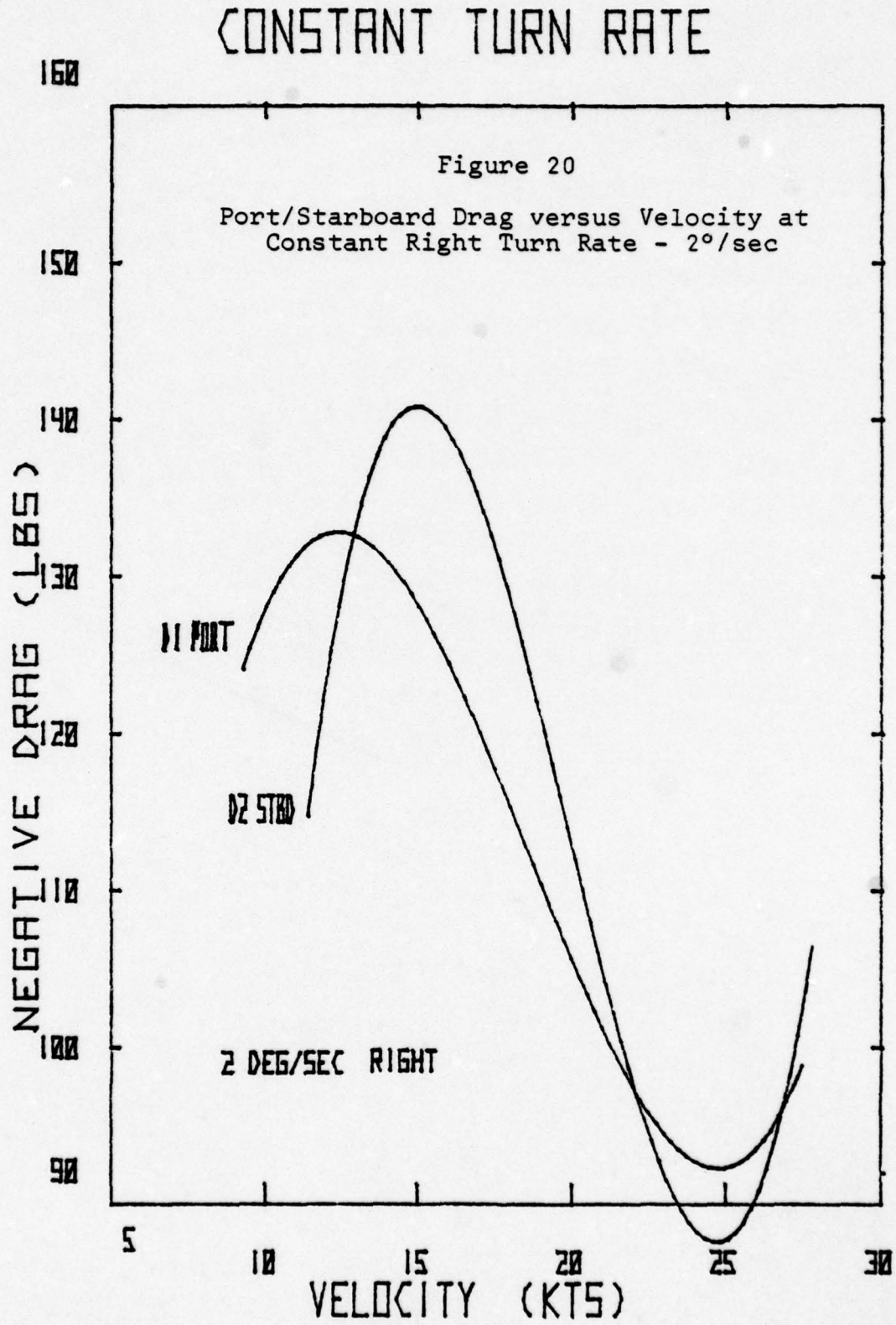

Figure 20

Port/Starboard Drag versus Velocity at Constant Right Turn Rate - 2°/sec

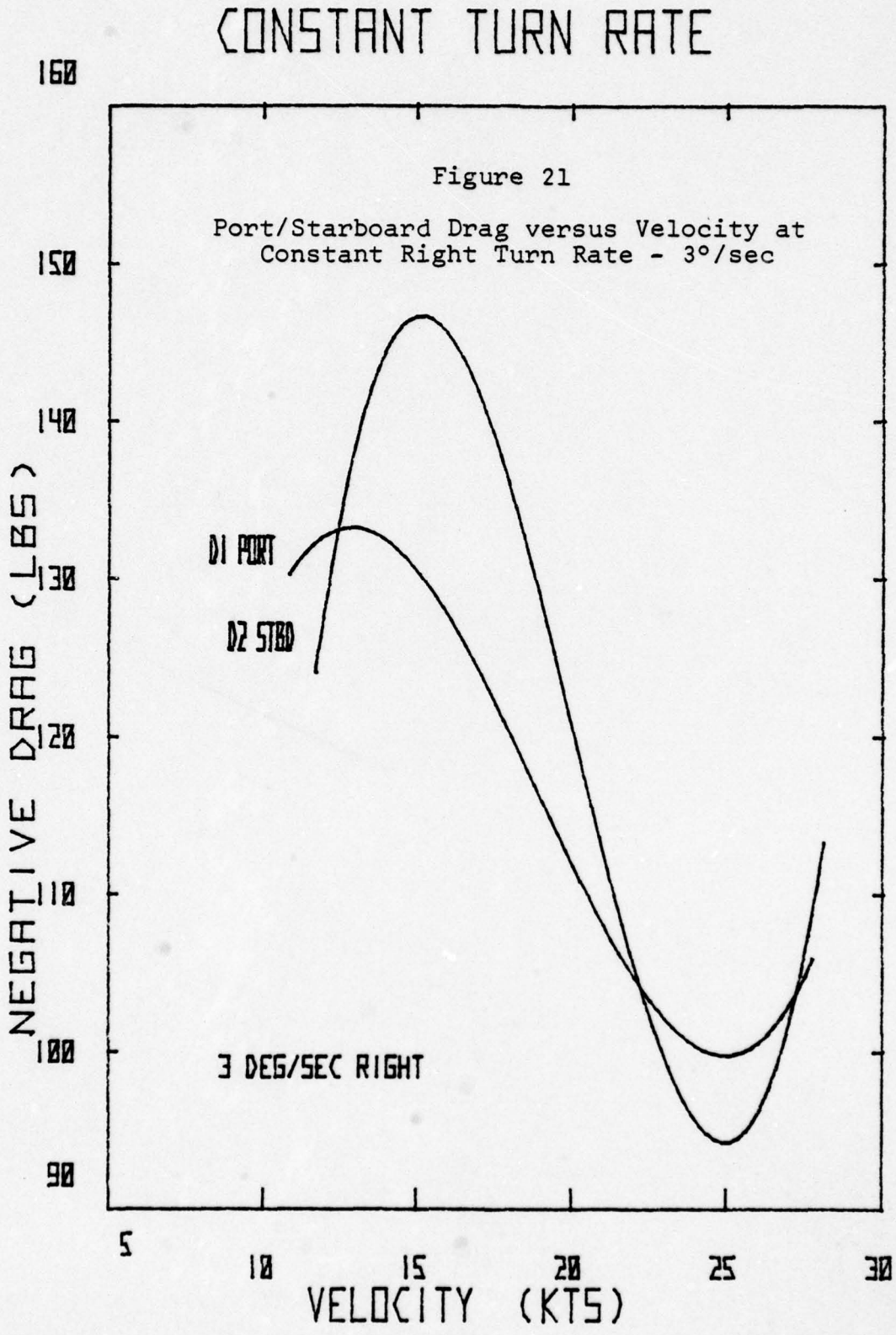

Figure 21

Port/Starboard Drag versus Velocity at Constant Right Turn Rate - 3°/sec

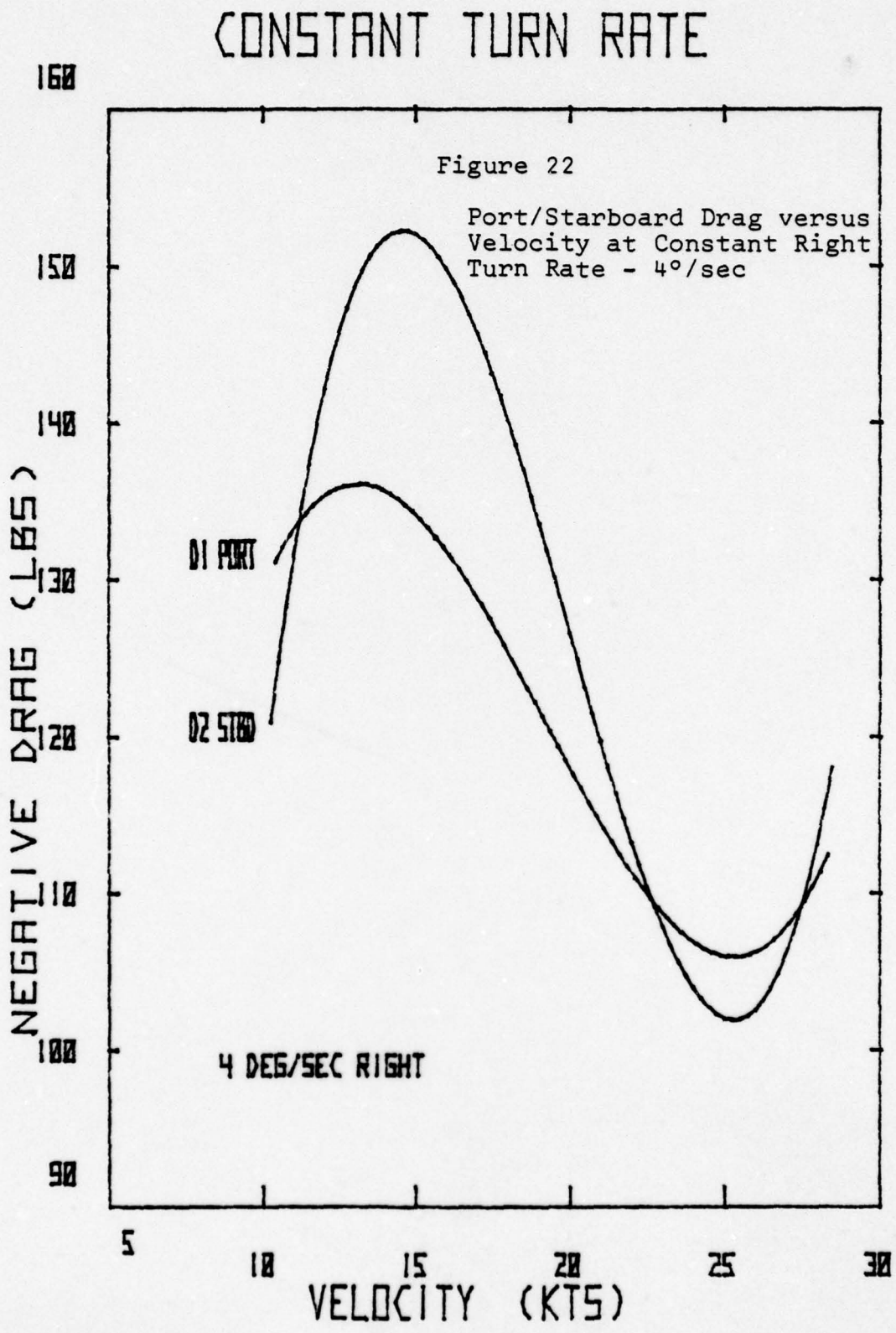

Figure 22

Port/Starboard Drag versus Velocity at Constant Right Turn Rate - 4°/sec

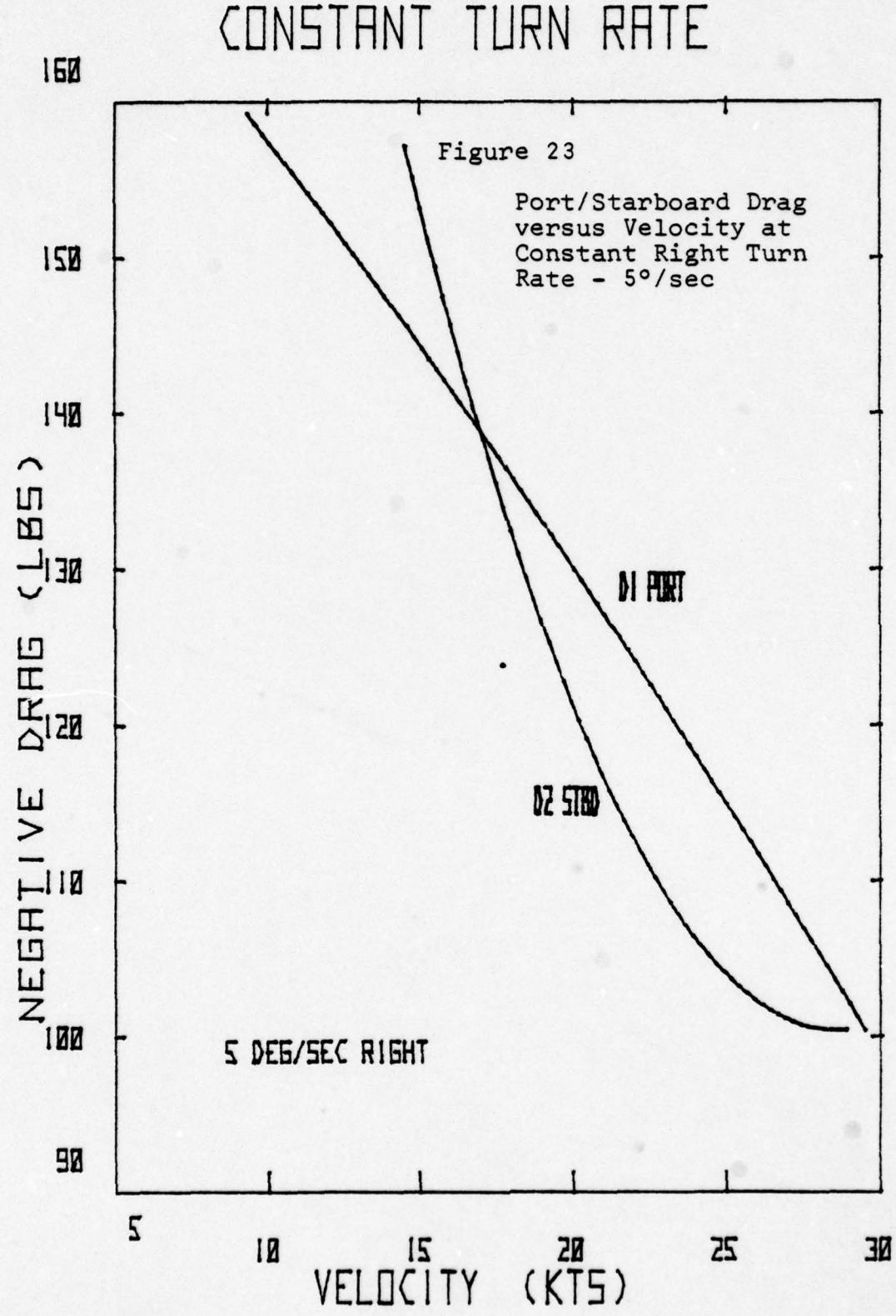
CONSTANT TURN RATE
160
150
140
130
120
110
100
90
NEGATIVE DRAG (LBS)
Figure 23
Port/Starboard Drag versus Velocity at Constant Right Turn Rate - 5°/sec
D1 PORT
D2 STBD
5 DEG/SEC RIGHT
5
10
15
20
25
30
VELOCITY (KTS)

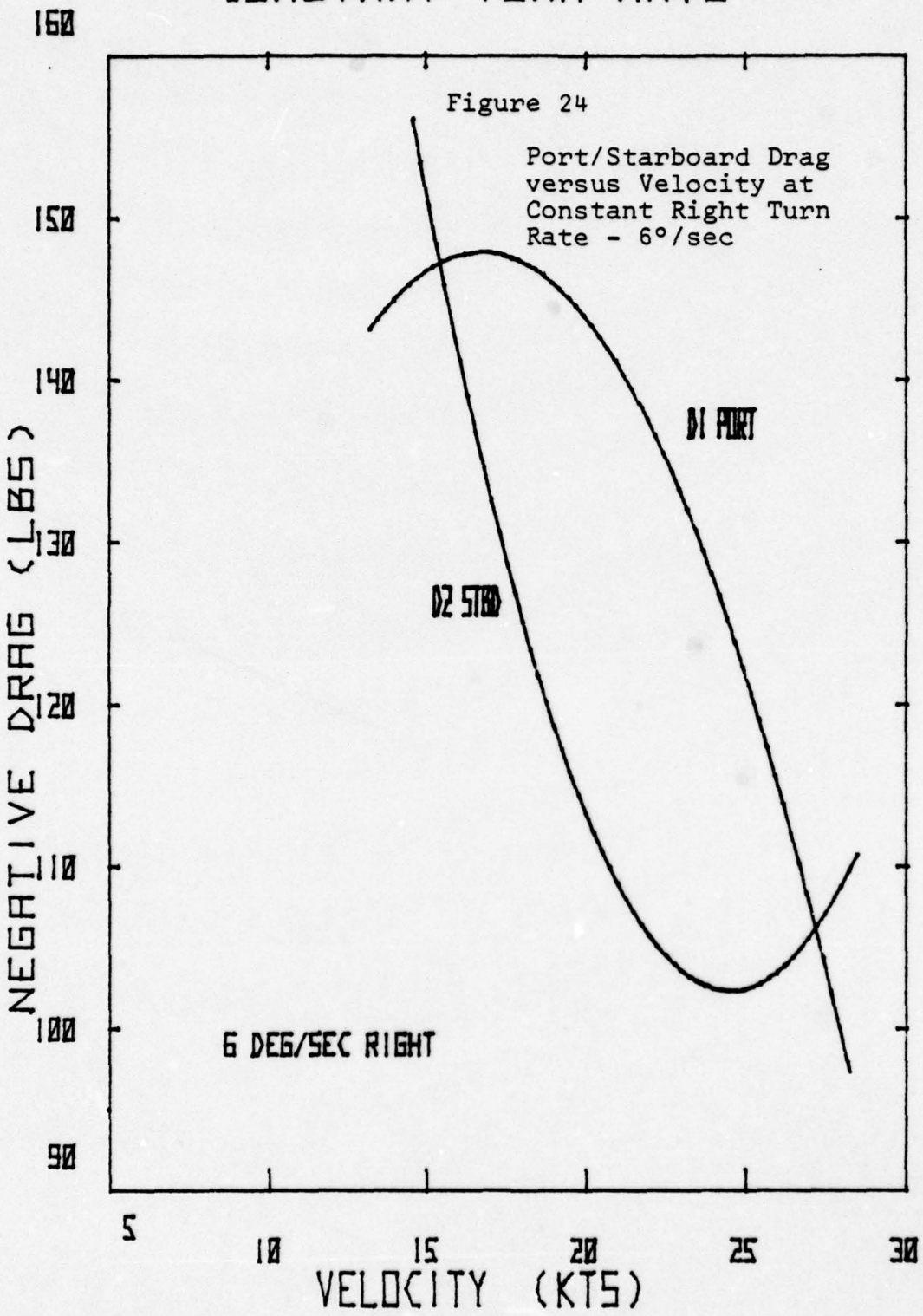

Figure 24

Port/Starboard Drag versus Velocity at Constant Right Turn Rate - 6°/sec

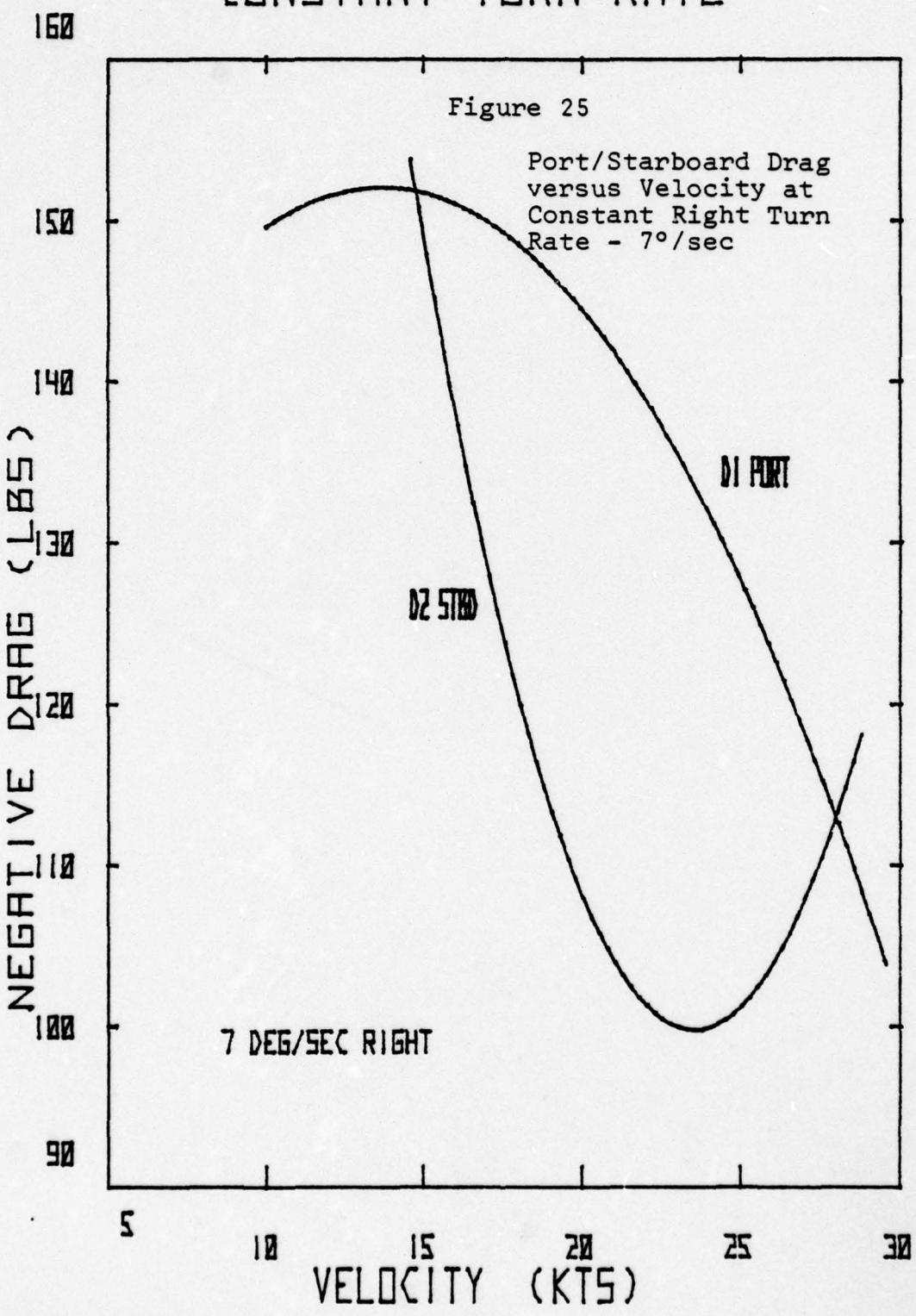
CONSTANT TURN RATE
160
150
140
130
120
110
100
90
NEGATIVE DRAG (LBS)
Port/Starboard Drag
versus Velocity at
Constant Right Turn
Rate - 7°/sec
D1 PORT
D2 STBD
7 DEG/SEC RIGHT
5
10
15
20
25
30
VELOCITY (KTS)

Figure 25

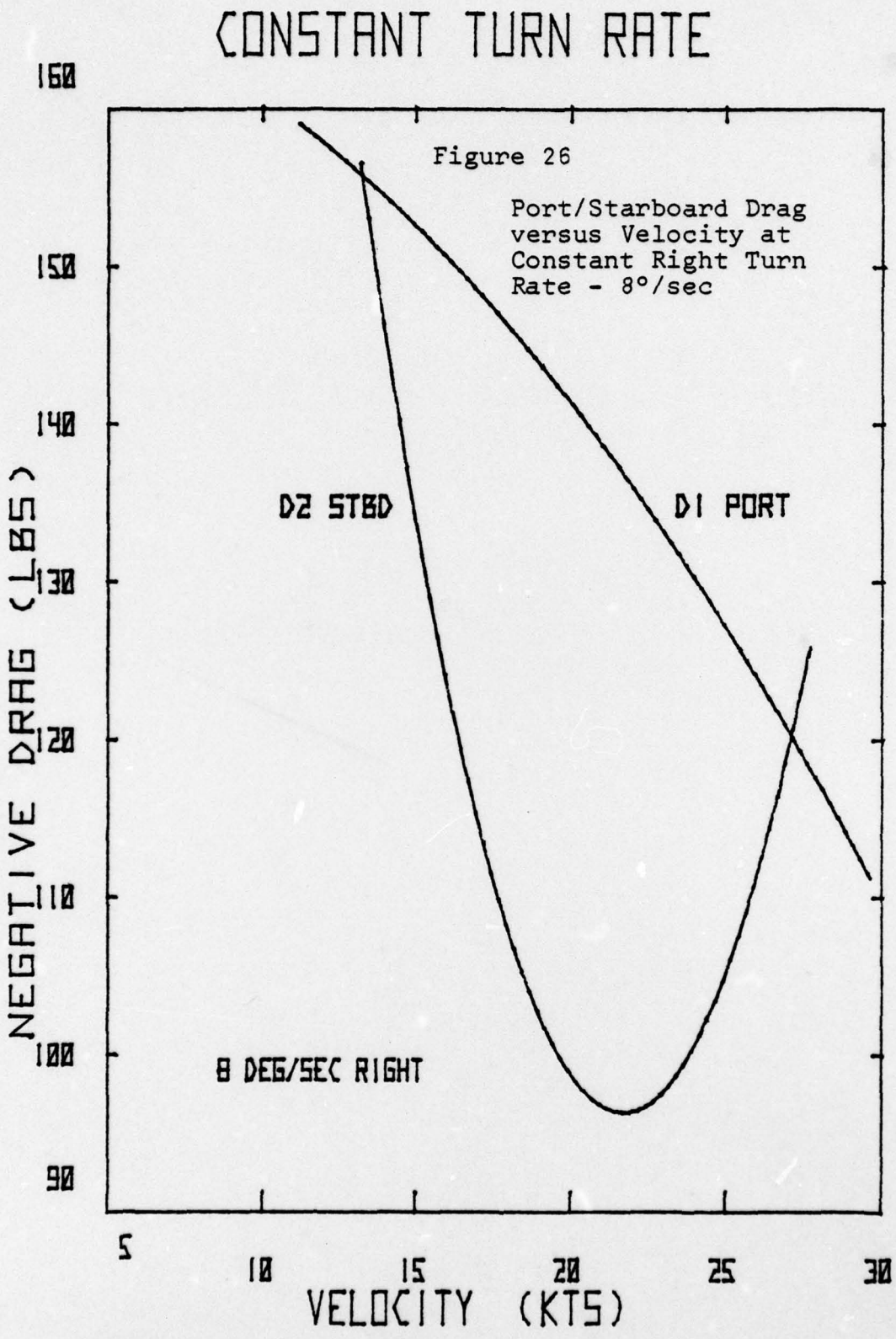

Figure 26

Port/Starboard Drag versus Velocity at Constant Right Turn Rate - 8°/sec

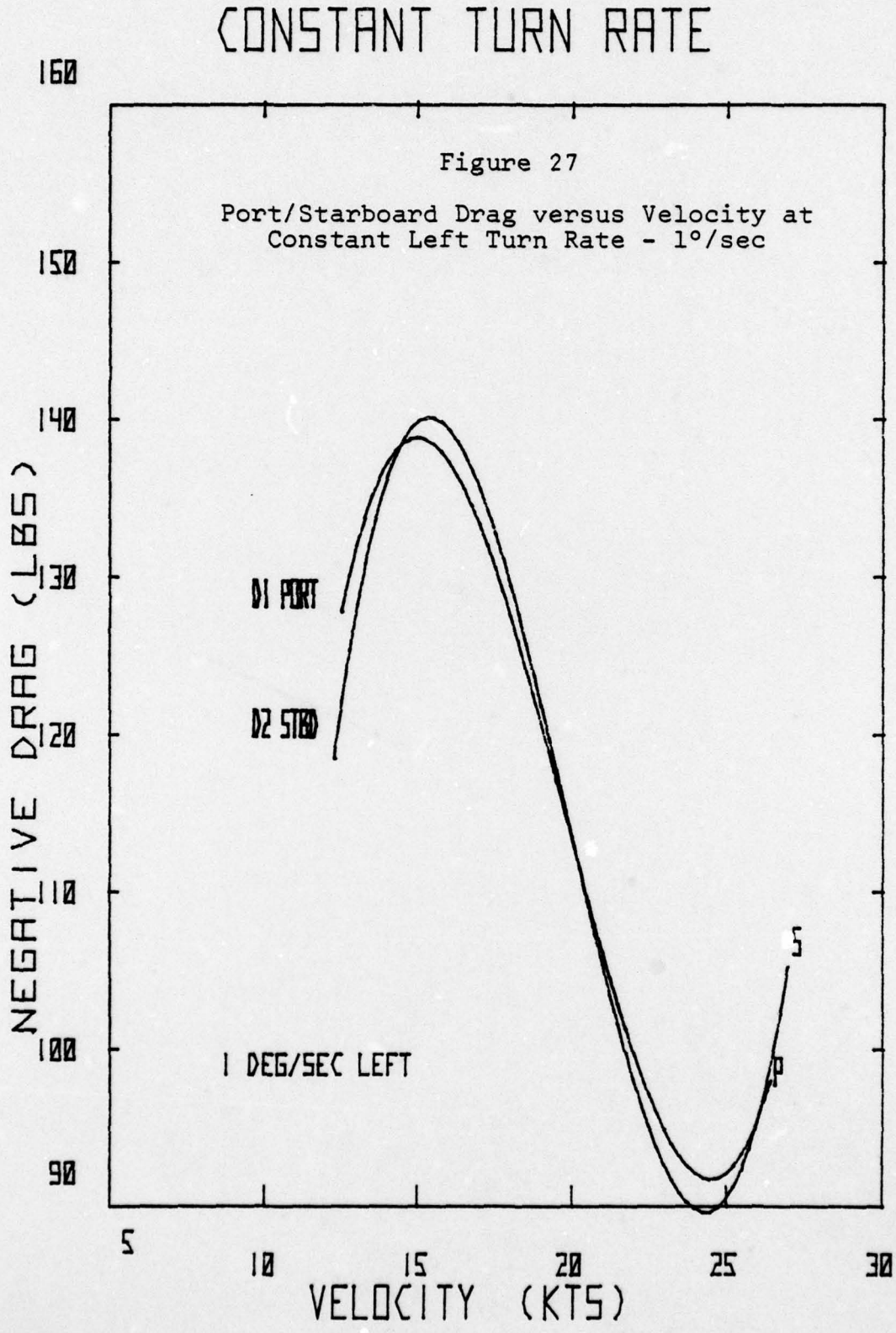

Figure 27

Port/Starboard Drag versus Velocity at Constant Left Turn Rate - 1°/sec

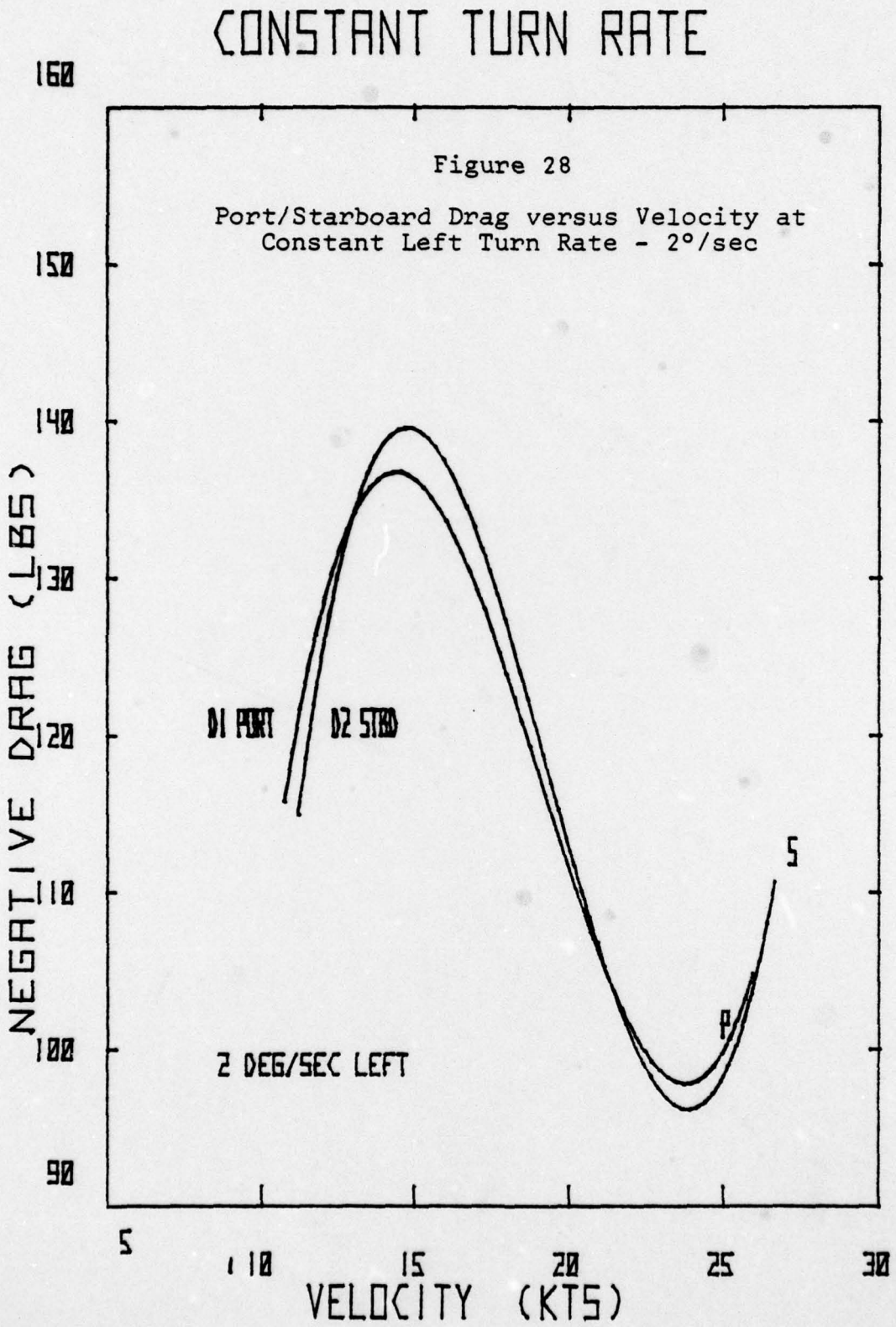

Figure 28

Port/Starboard Drag versus Velocity at Constant Left Turn Rate - 2°/sec

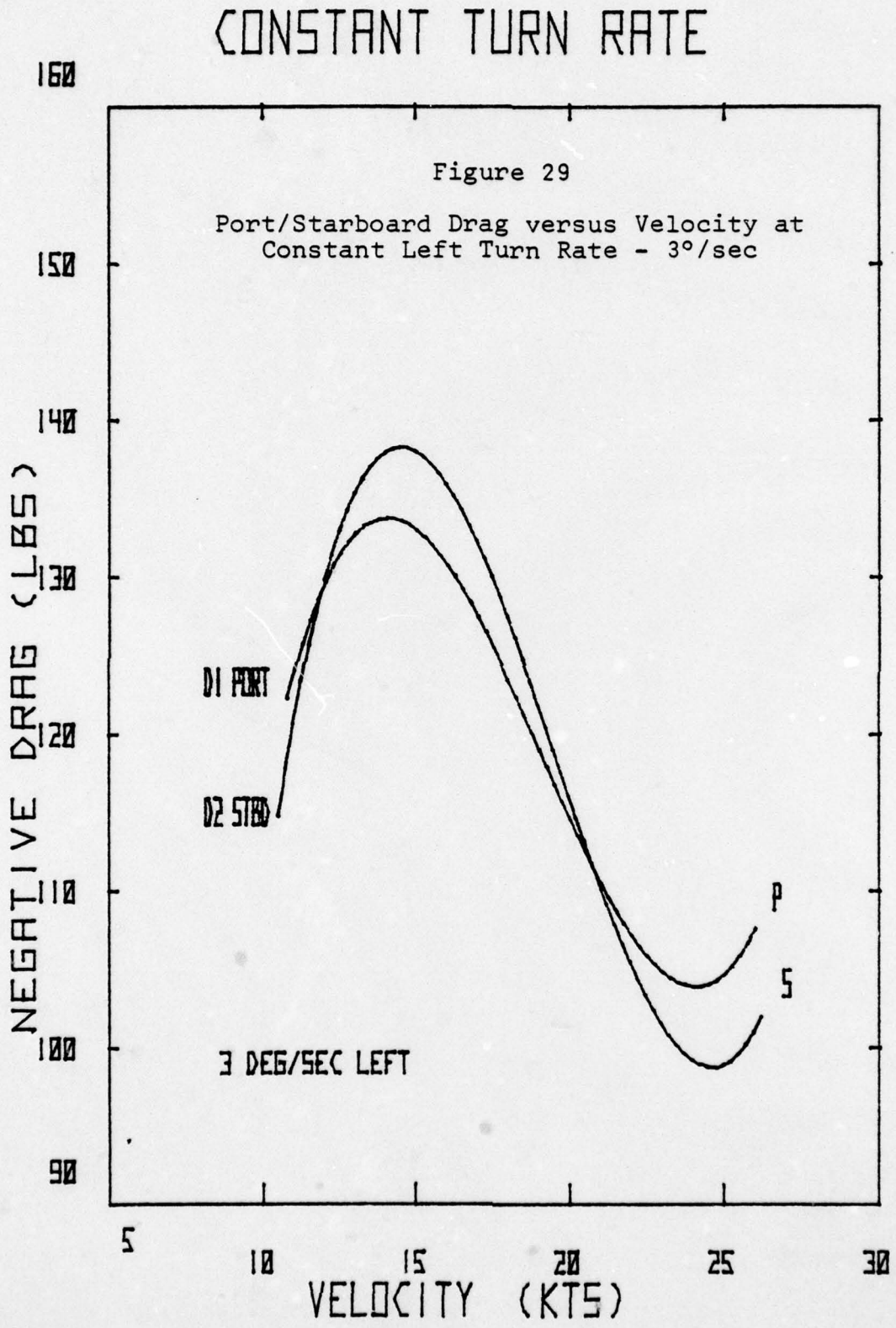

Figure 29

Port/Starboard Drag versus Velocity at Constant Left Turn Rate - 3°/sec

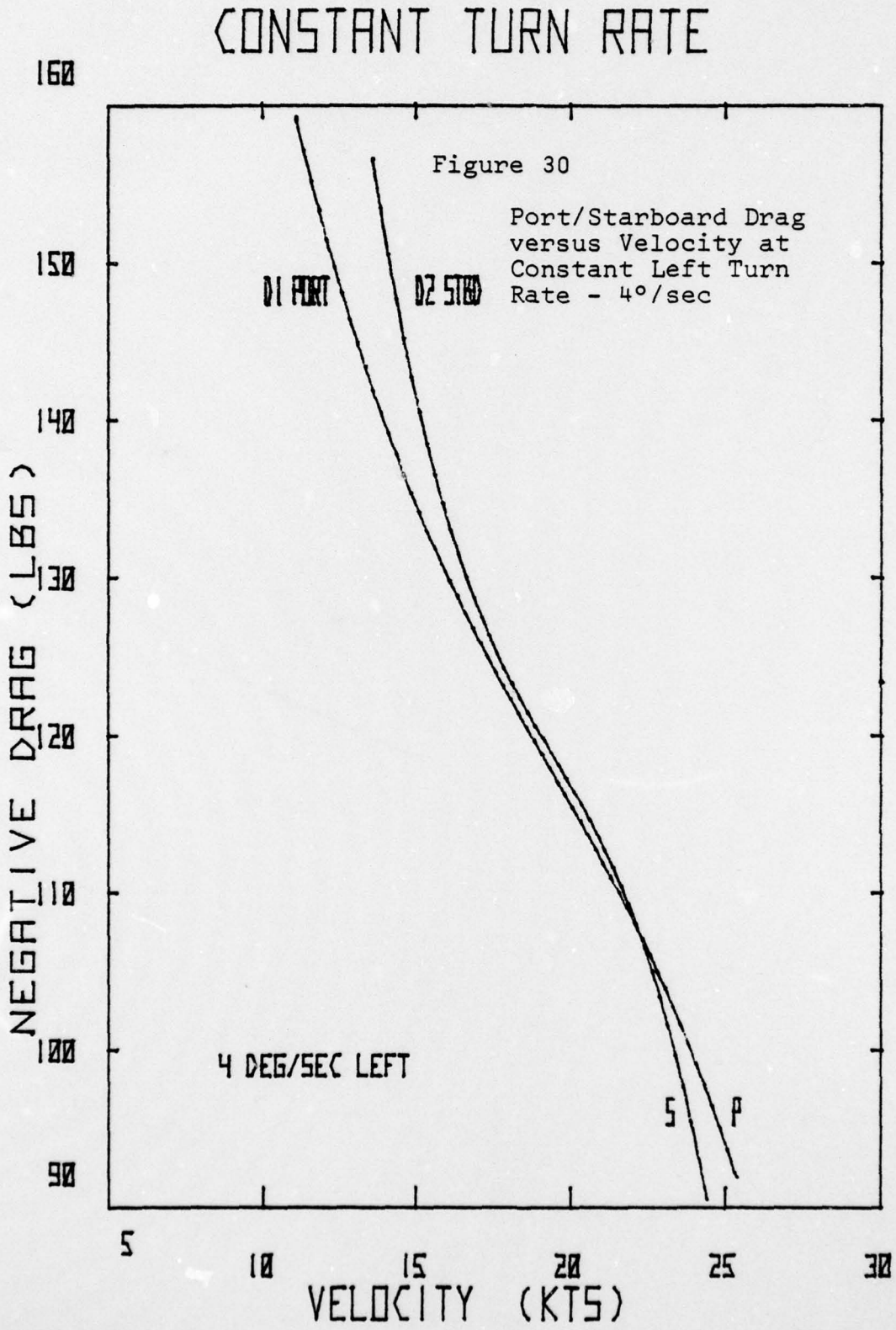

Figure 30

Port/Starboard Drag versus Velocity at Constant Left Turn Rate - 4°/sec

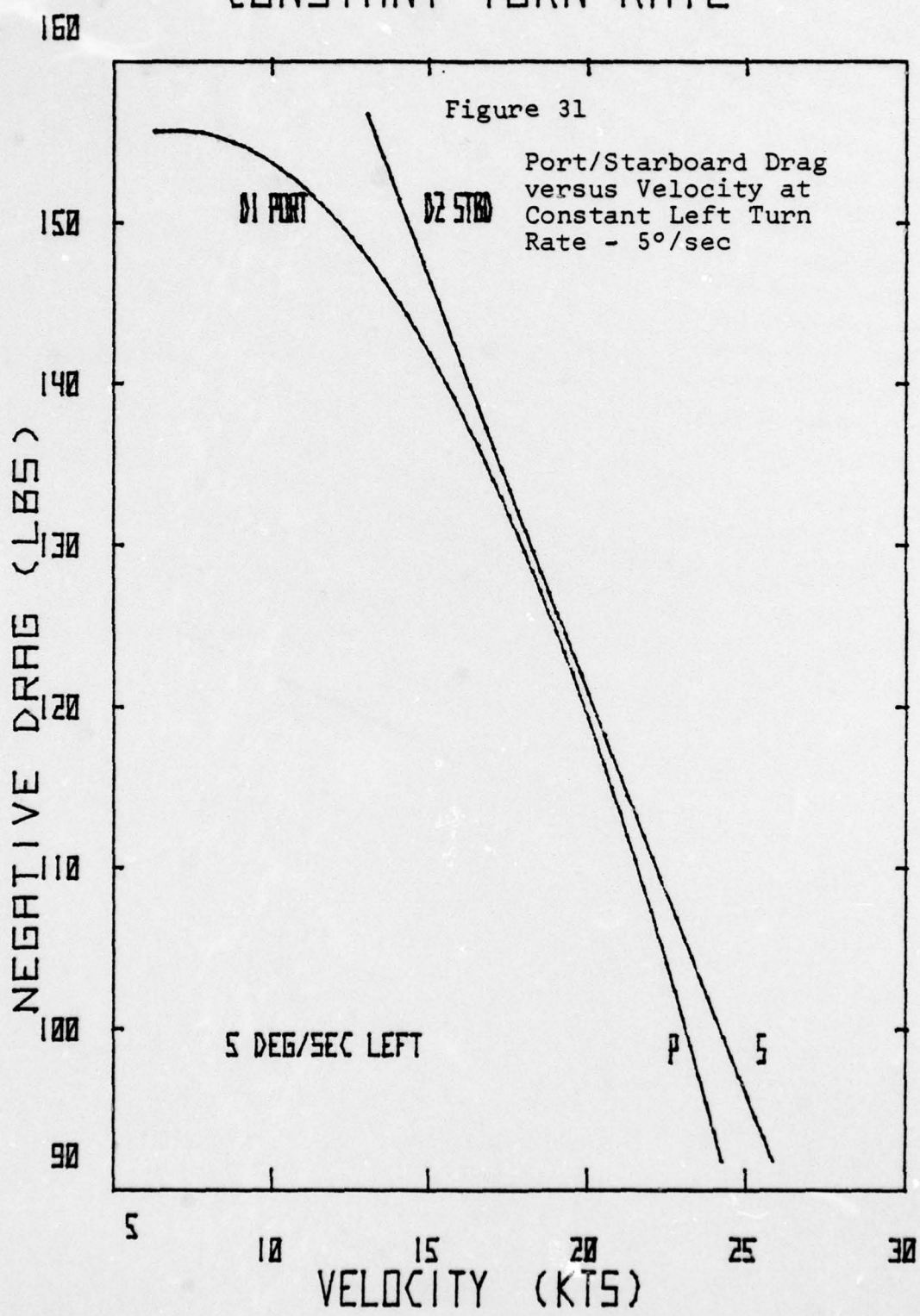

Figure 31

Port/Starboard Drag versus Velocity at Constant Left Turn Rate - 5°/sec

Figure 32

Summary Differential Drag Data Table

Turn Rate (deg/sec)	Testcraft Velocity (kts) 10.	11.	12.	13.	14.	15.	16.	17.	18.	19.
1R	-	-	-	5	-4	-10	-13	-14	-13	-12
2R	-	-	10	-1	-9	-13	-15	-15	-13	-10
3R	-	-	4	-7	-13	-16	-18	-17	-15	-11
4R	-	2	-7	-13	-16.5	-18	-18	-18	-14	-11
5R	-	-	-	-	-	-9	-4	0	+4	+7
6R	-	-	-	-	-	-4	+7	+15	+23	+27
7R	-	-	-	-	-6	+2	+13	+21	+28	+33
8R	-	-	-	-2	+9	+18	+26	+33	+38	+42
1L	-	-	-	-4	-1	+1	+2	+2	+2	+1
2L	-	-	-3	0	+2	+4.3	+3.5	+3.5	+3	+2
3L	-	-4	0	+3	+4.3	+5	+5	+4.7	+3.6	+2
4L	-	-	-	-	+11	+6	+3.5	+1.8	+1	+1
5L	-	-	-	+9	+6.5	+4.5	+3	+2	+1.2	+1

Figure 32 (cont.)

Turn Rate (deg/sec)	Testcraft Velocity (kts) 20	21	22	23	24	25	26	27	28
1R	-9	-6	-3	0	+3	+4	+4	+2	-2
2R	-7	-3	0	+3	+5	+5	+3	-2	-
3R	-8	-4	0	+3	+5	+5	+4	0	-
4R	-8	-5	-2	+1	+3	+4	3.5	1	-
5R	+9	+10.5	+11	+11.5	+11	+11	+9	+7	-
6R	+30.5	+31.5	+32	+29	+24	+18	+10	0	-12
7R	+36	+38	+37	+35	+32	+25	+18	+9	0
8R	+42.5	+43	+39	+35	+29	+20	+11	0	
1L	0	-1	-1.6	-2.1	-2.2	-1.5	0	0	-
2L	+1	0	-.8	-1.3	-1.8	-1.5	0	0	-
3L	+1	-.8	-2	-3.5	-5	-6	-5.5	-	-
4L	+1	+.8	0	-1.5	-5	-	-	-	-
5L	+1.5	+2.5	+3.5	+5	+7.2	-	-	-	-

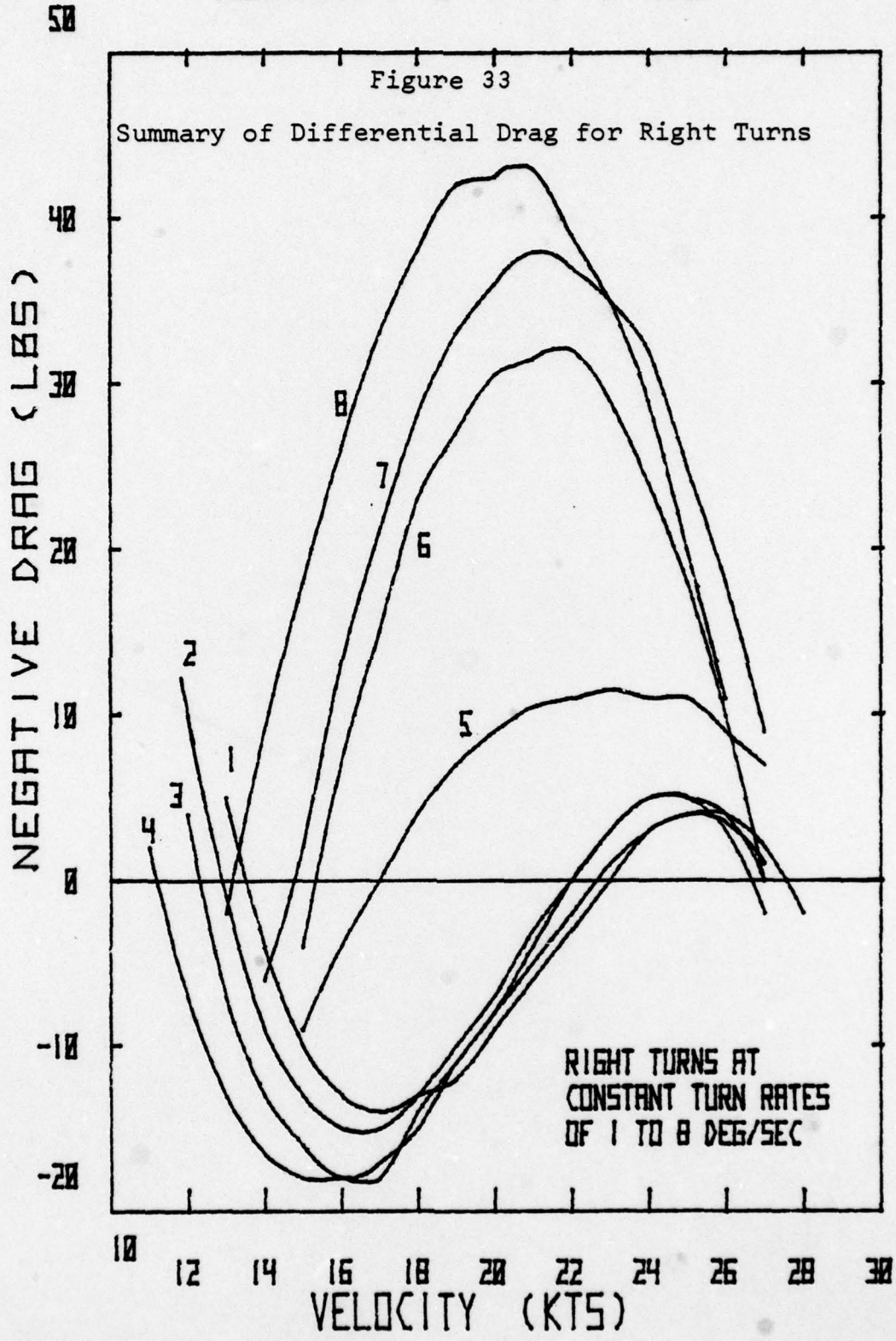

Figure 33

Summary of Differential Drag for Right Turns

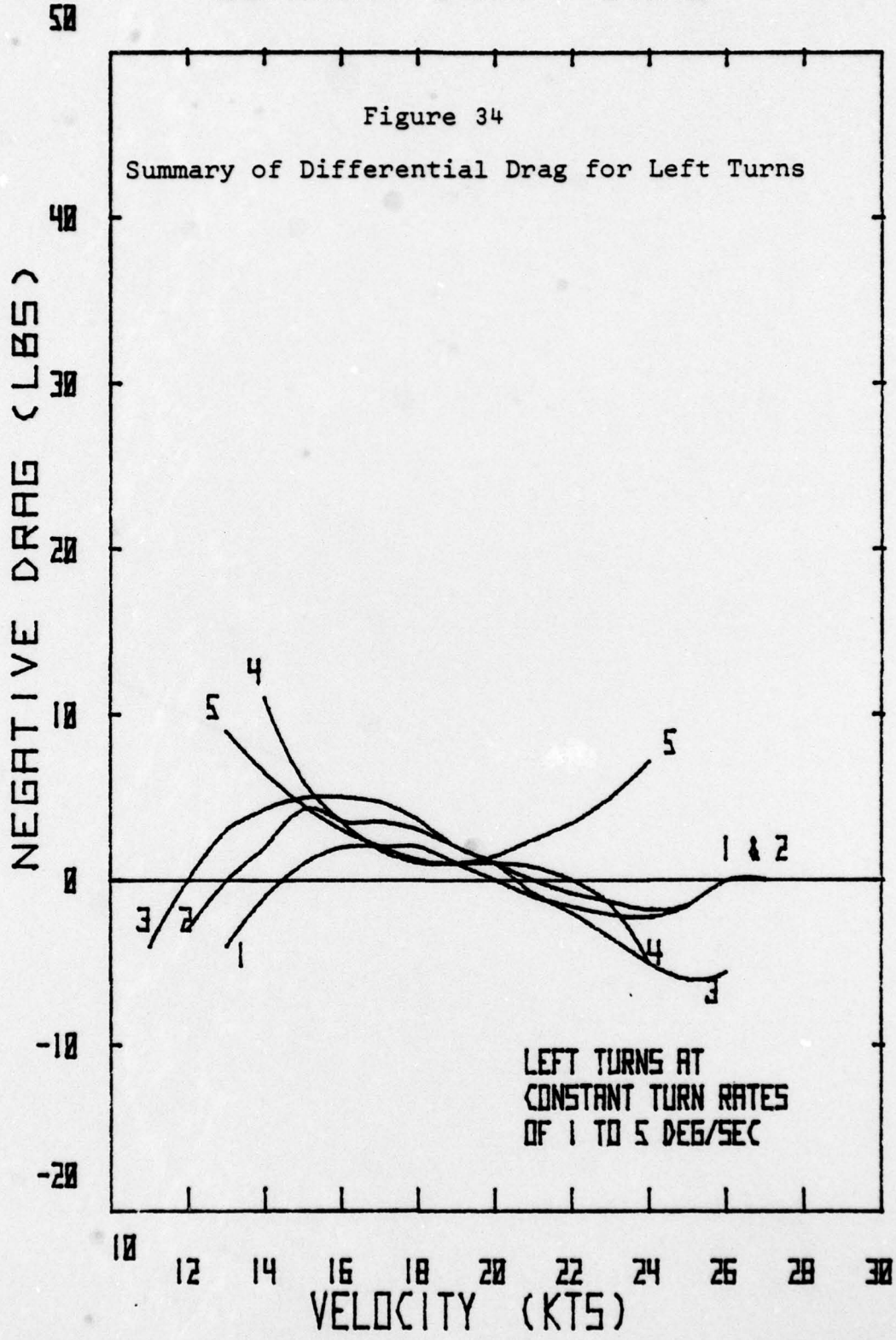

Figure 34

Summary of Differential Drag for Left Turns

DIFF. DRAG SENSE

Figure 35

RIGHT TURNS "Sense" of Differential Drag for Right Turns

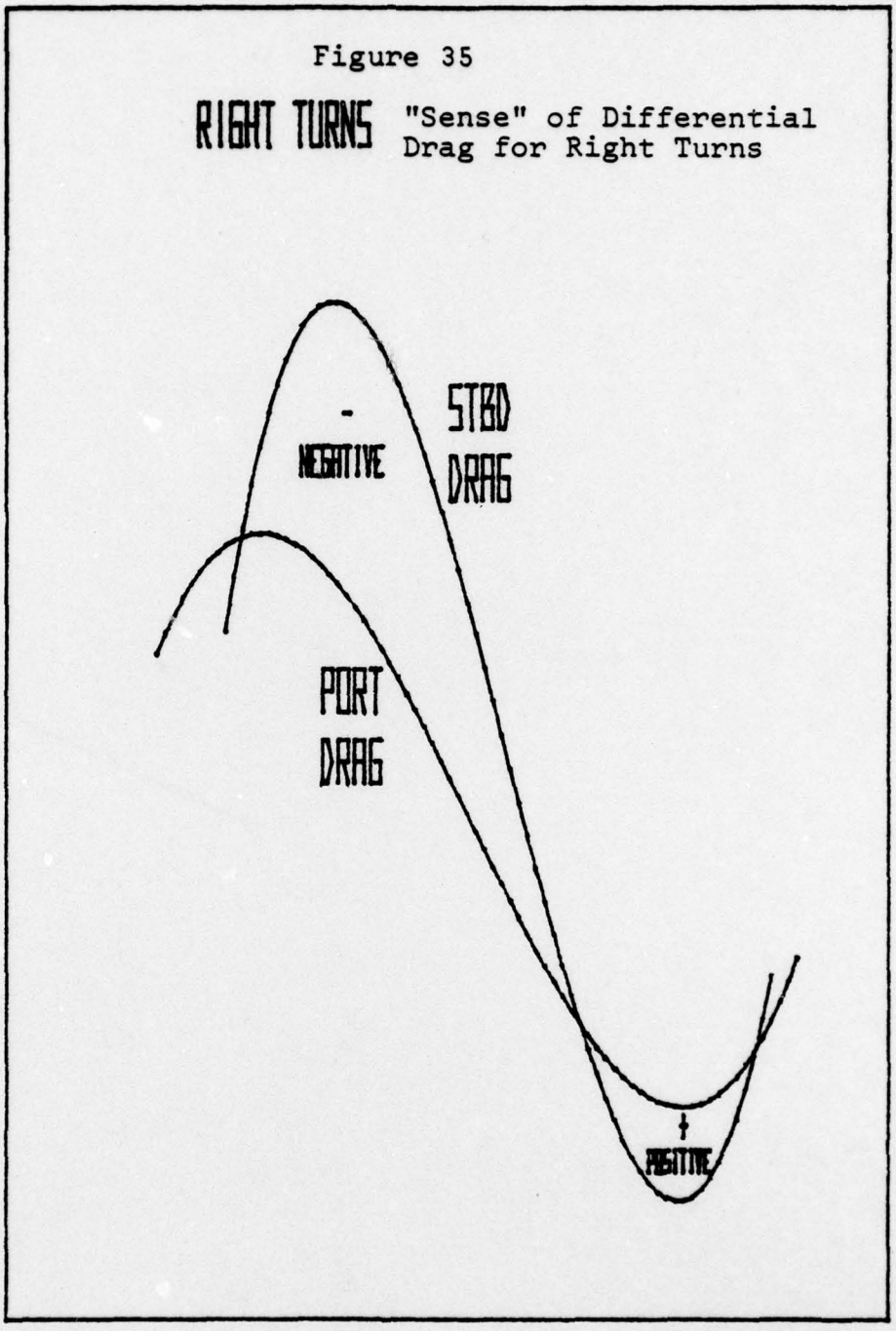

DIFF. DRAG SENSE

Figure 36

LEFT TURNS "Sense" of Differential Drag for Left Turns

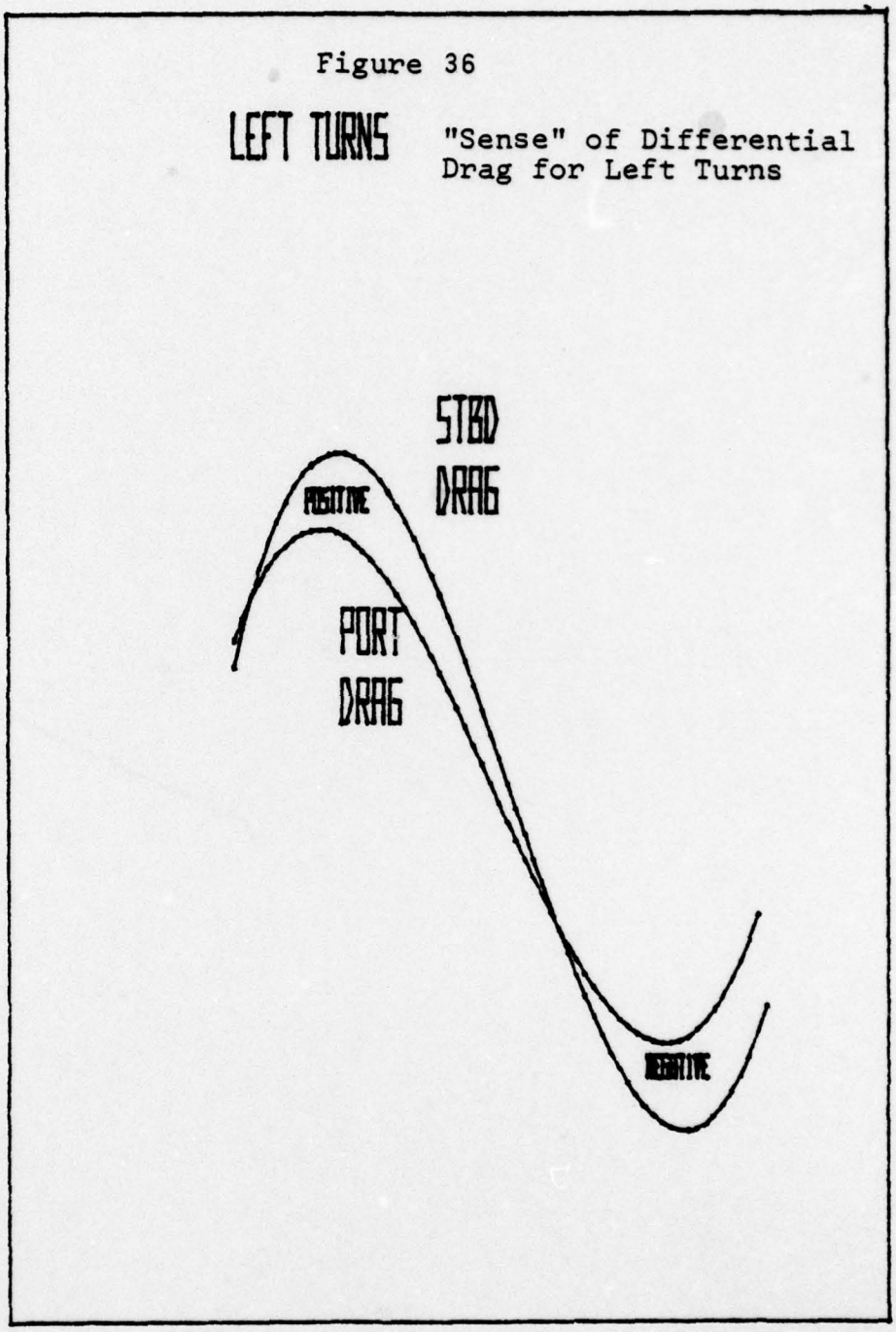

LIST OF REFERENCES

1. Alferi, Paul A., Lift and Drag Analysis on the Bow Seal of the Surface Effect Testcraft XR-3, M.S. Thesis, Naval Postgraduate School, Monterey, California, September 1977.

2. Boland, James A., Lift and Drag Measurement and Analysis of the Stern Seal of the Captured Air Bubble Testcraft XR-3, M.S. Thesis, Naval Postgraduate School, Monterey, California, March 1977.

3. Dabbieri, Peter V. Jr., Data Reduction System for the XR-3 Captured Air Bubble Testcraft, M.S. Thesis, Naval Postgraduate School, Monterey, California, December 1977.

4. David W. Taylor Naval Ship Research and Development Center Report 77-0056, An Analysis of Seal Loads and Their Effect on the Performance of a Surface Effect Ship in Calm Water, by Charles E. Heber, Jr., December 1977.

5. Jane's Surface Skimmers, Hovercraft and Hydrofoils, 1978, p.371, Macdonald and Jane's Publishing Ltd., London.

6. Layton, Donald M., Seal Loads of the Surface Effect Ship Testcraft XR-3, NPS67-78-001PR, Naval Postgraduate School, Monterey, California, November 1977.

7. Roberts, James H., XR-3 Turning Performance, M.S. Thesis, Naval Postgraduate School, Monterey, California, December 1974.

INITIAL DISTRIBUTION LIST

		No. Copies
1.	Defense Documentation Center Cameron Station Alexandria VA 22314	2
2.	Library, Code 0142 Naval Postgraduate School Monterey CA 93940	2
3.	Chairman, Aeronautical Engineering Dept. Code 67 Naval Postgraduate School Monterey CA 93940	1
4.	Chairman, Mechanical Engineering Dept. Code 69 Naval Postgraduate School Monterey CA 93940	1
5.	David W. Taylor Naval Ship Research and Development Center Code 163 Bethesda MD 20084	1
6.	Naval Sea Systems Command PMS 304-31 P.O. Box 34401 Bethesda MD 20034	1
7.	Assoc. Professor Donald M. Layton Code 69Ln Naval Postgraduate School Monterey CA 93940	5
8.	LCDR David A. Edwards, USN 3911 9th Avenue S.W. Huntsville AL 35805	1